Accessing the coupled-channels dynamics using femtoscopic correlations at LHC

V. Mantovani Sarti (TUM)

THEIA Strong seminar – 08.12.2021

Deutsche Forschungsgemeinschaft

Coupled-channel dynamics in h-h interactions

- Coupled-channel dynamics widely present in hadron-hadron strong interactions
  - Close in mass and same quantum numbers (e.g. B,S,Q)
  - On-shell and off-shell processes from one channel to the other

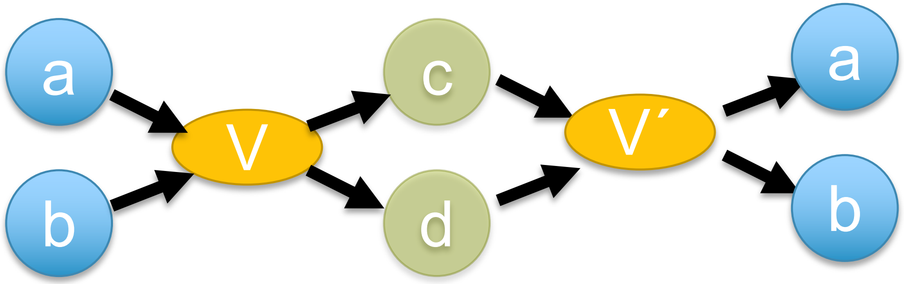

Coupled-channel dynamics in h-h interactions

- Coupled-channel dynamics widely present in hadron-hadron strong interactions
  - Close in mass and same quantum numbers (e.g. B,S,Q)
  - On-shell and off-shell processes from one channel to the other

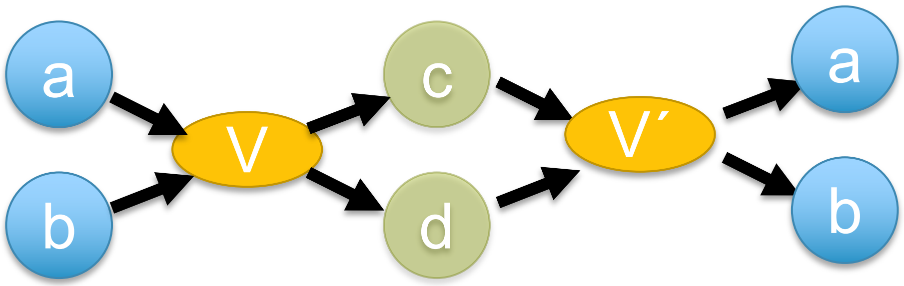

- Constraints on inelastic part crucial for:
  - existence of bound states
    - di-baryon
  - nature of resonances
    - hadron molecules
    - exotic hadrons (pentaquarks,…)

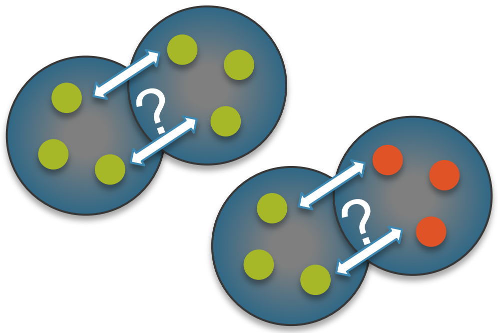

- NΩ, ΩΩ, ΛΛ, $B\bar{B}$, …

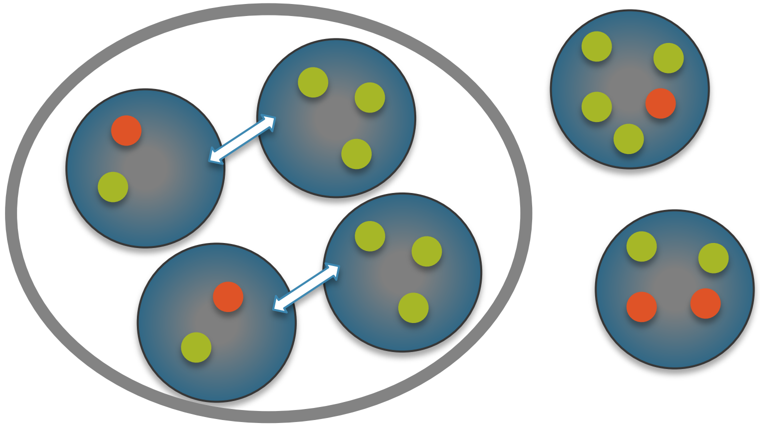

- Λ(1405) in $\bar{K}N$, charmonium states, …

Coupled-channels in scattering experiments

- Fixed initial state (e.g K⁻) and different final states:
  - elastic scattering: 1→1
  - inelastic scattering: 1→2,3…

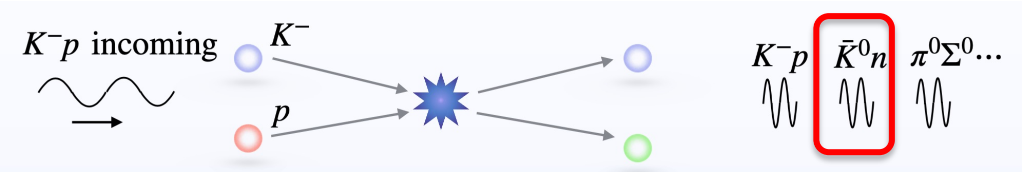

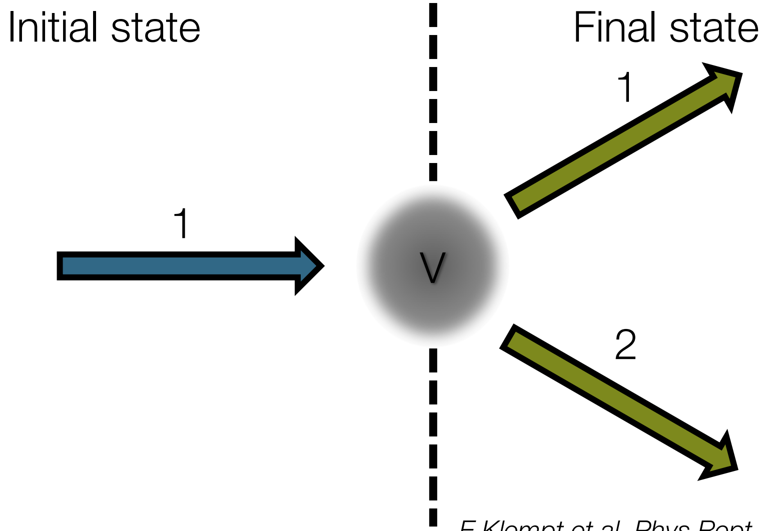

- Measurement of the cross-section in different channels

- Disadvantages:
  - not accessible down to zero momenta
  - large uncertainties
  - limited to few h-h interactions

G.S. Abrams et al. Phys.Rev. 139 (1965) B454-B457

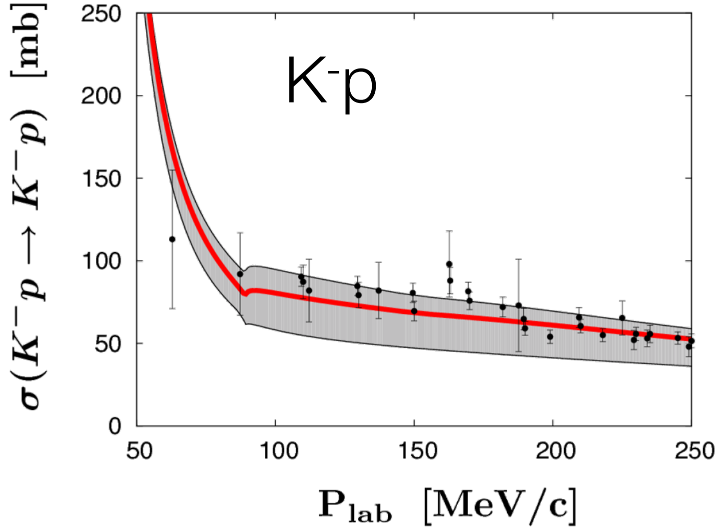

E.Klempt et al. Phys.Rept. 368 (2002) 119-316

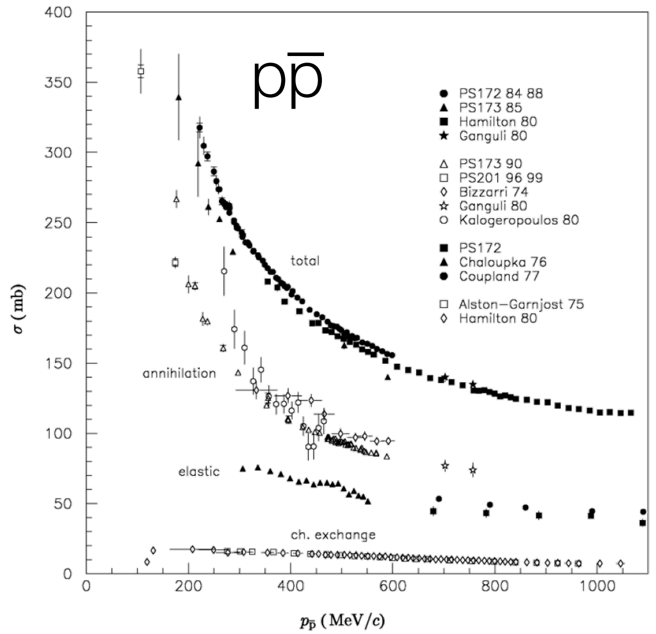

Coupled-channels in femtoscopy

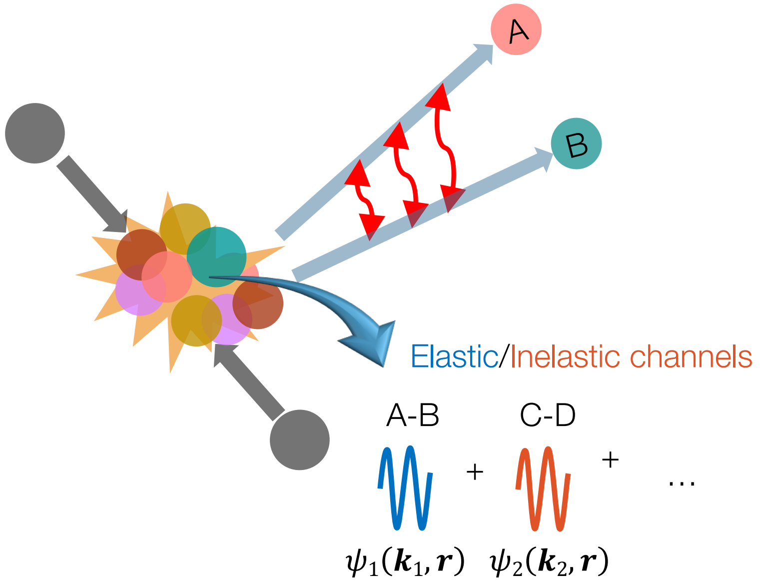

- Conversion weights w_j
  - produced pairs in j channel as initial states → yields + kinematics
    - thermal models and transport models

$$C_{A-B}(k^*) = \int S(r)\ |\psi_{1\to1}(k^*, r)|^2\, d^3r + \sum_{j\neq1} w_j^{prod} \int S_j(r)\ \left|\psi_{j\to1}(k_j{}^*, r)\right|^2 d^3r = \mathcal{N}(k^*)\frac{N_{same}(k^*)}{N_{mixed}(k^*)}$$

elastic
A-B → A-B

inelastic
C-D → A-B, …

Femtoscopy in ALICE

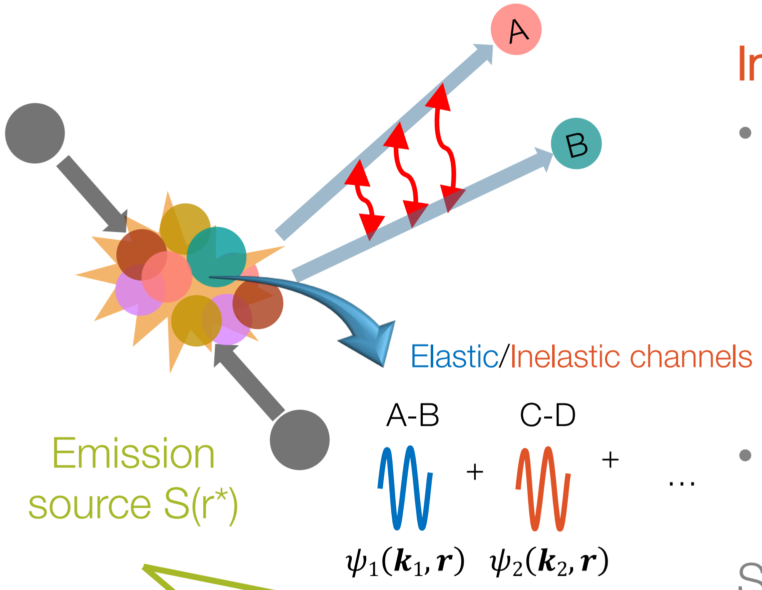

In small colliding systems:

- Gaussian r_{core} + resonance source model anchored to known interactions
  - Universal emitting source for particles
- Effective Gaussian with r_G ~1-2 fm

See more in Dimitar´s talk

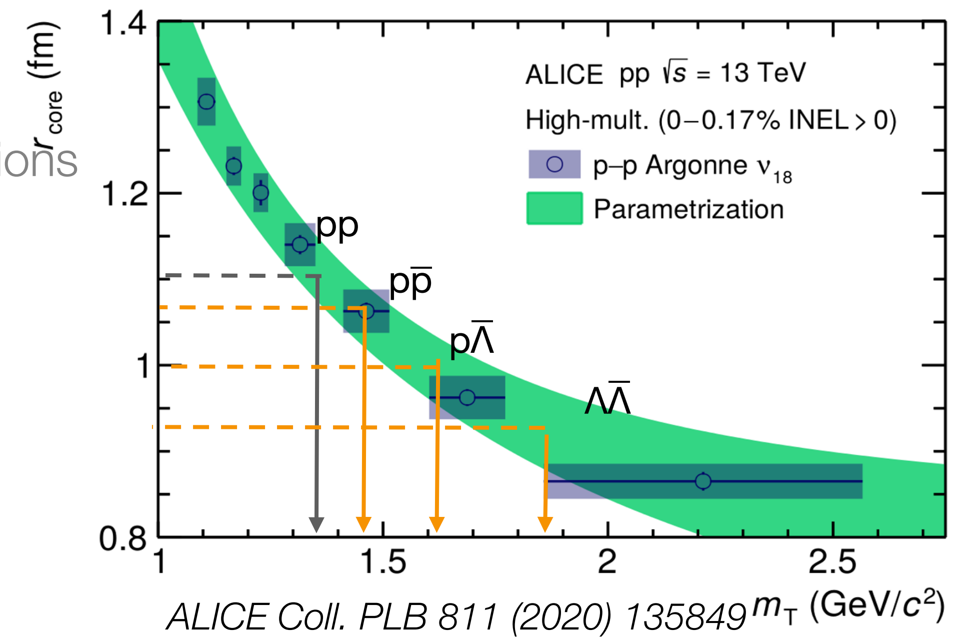

$$C_{A-B}(k^*) = \int S(r)\,|\psi_{1\to1}(k^*, r)|^2\, d^3r + \sum_{j\neq1} w_j^{prod} \int S_j(r)\, \left|\psi_{j\to1}(k_j^*, r)\right|^2 d^3r = \mathcal{N}(k^*)\,\frac{N_{same}(k^*)}{N_{mixed}(k^*)}$$

elastic
A-B → A-B

inelastic
C-D → A-B, …

Femtoscopy in ALICE

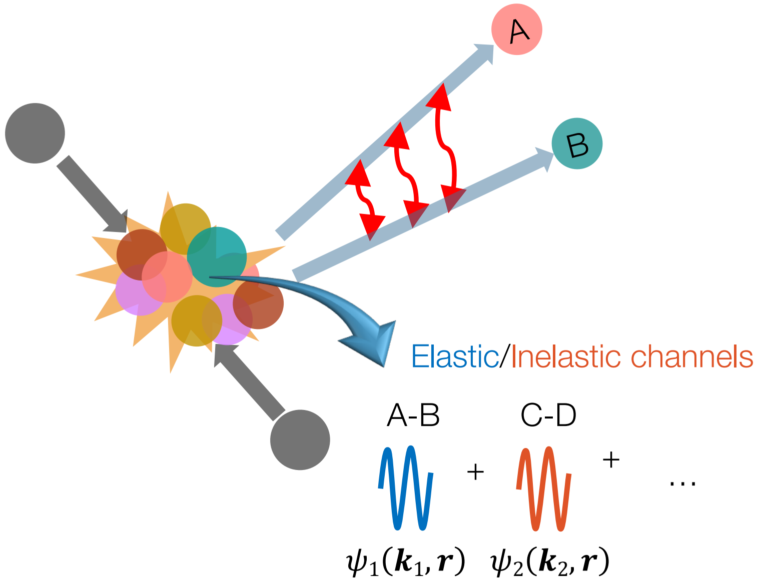

(from Dr. Y. Kamiya´s talk at AW Dec.2021)

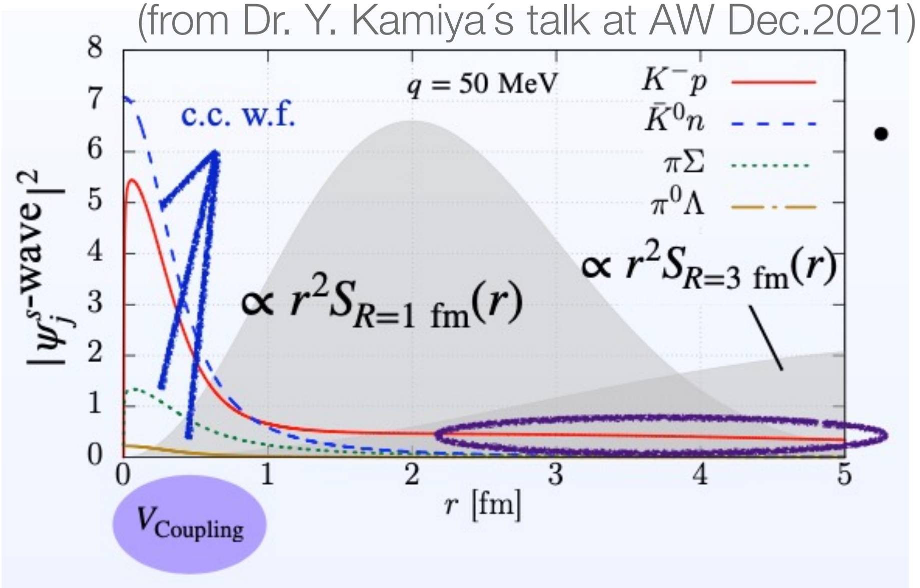

- Coupled-channel wfs playing a role at low distances

Elastic/Inelastic wave functions

$$C_{A-B}(k^*) = \int S(r)\,|\psi_{1\to1}(k^*, r)|^2\, d^3r + \sum_{j\neq1} w_j^{prod} \int S_j(r)\,|\psi_{j\to1}(k_j^*, r)|^2\, d^3r = \mathcal{N}(k^*)\frac{N_{same}(k^*)}{N_{mixed}(k^*)}$$

elastic
A-B → A-B

inelastic
C-D → A-B, …

Femtoscopy in ALICE

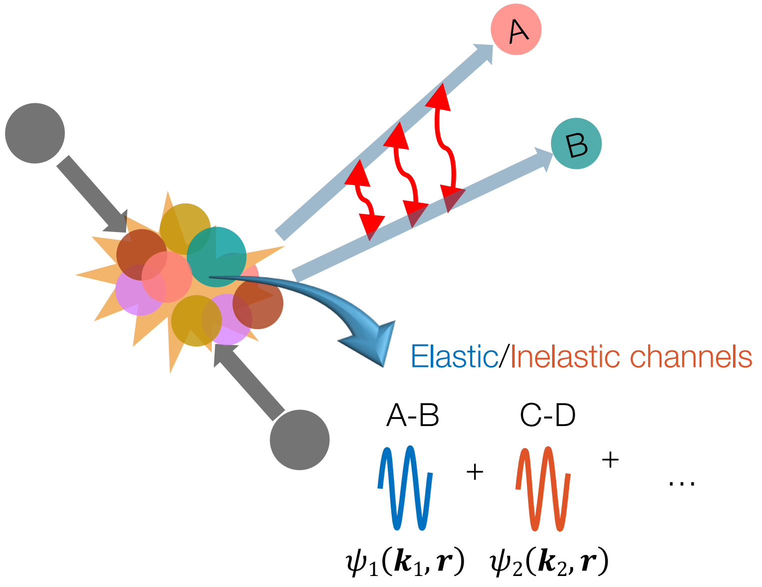

Correlation function

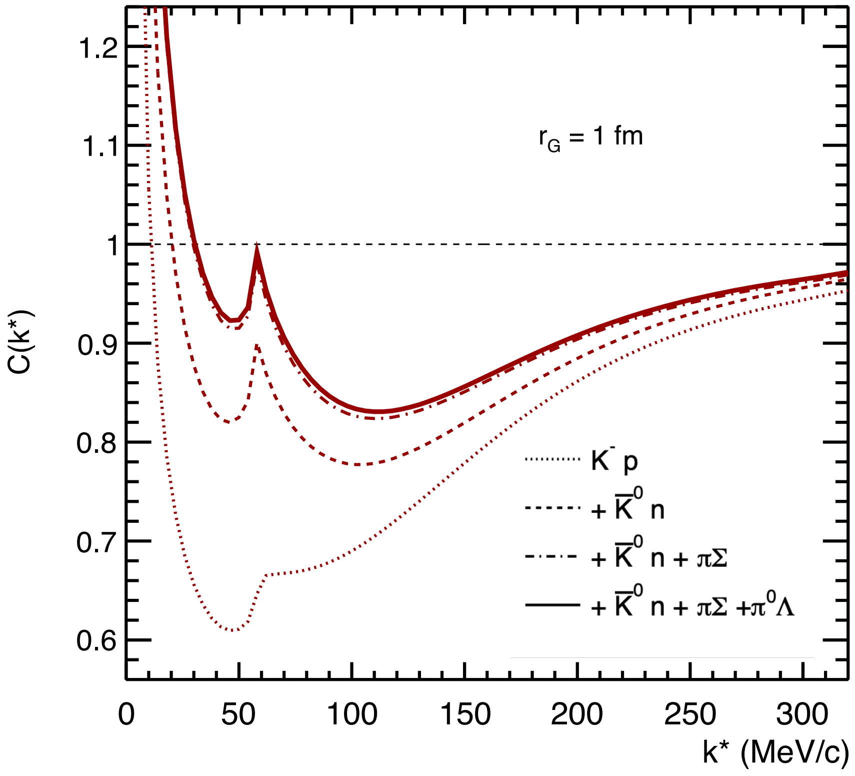

$$C_{A-B}(k^*) = \int S(r)\ |\psi_{1\to1}(k^*, r)|^2\, d^3r + \sum_{j\neq1} w_j^{prod} \int S_j(r)\ |\psi_{j\to1}(k_j^*, r)|^2 d^3r = \mathcal{N}(k^*)\frac{N_{same}(k^*)}{N_{mixed}(k^*)}$$

elastic
A-B → A-B

inelastic
C-D → A-B, …

J. Haidenbauer Nucl.Phys.A 981 (2019)
Y. Kamiya et al. Phys.Rev.Lett. 124 (2020)
V.M.S., L. Fabbietti, O. Vazquez-Doce 2012.09806

Femtoscopy in ALICE

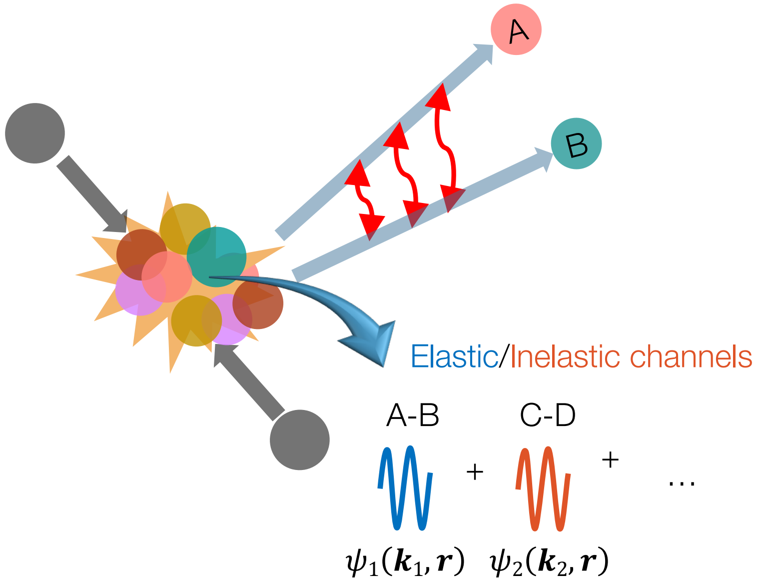

Correlation function

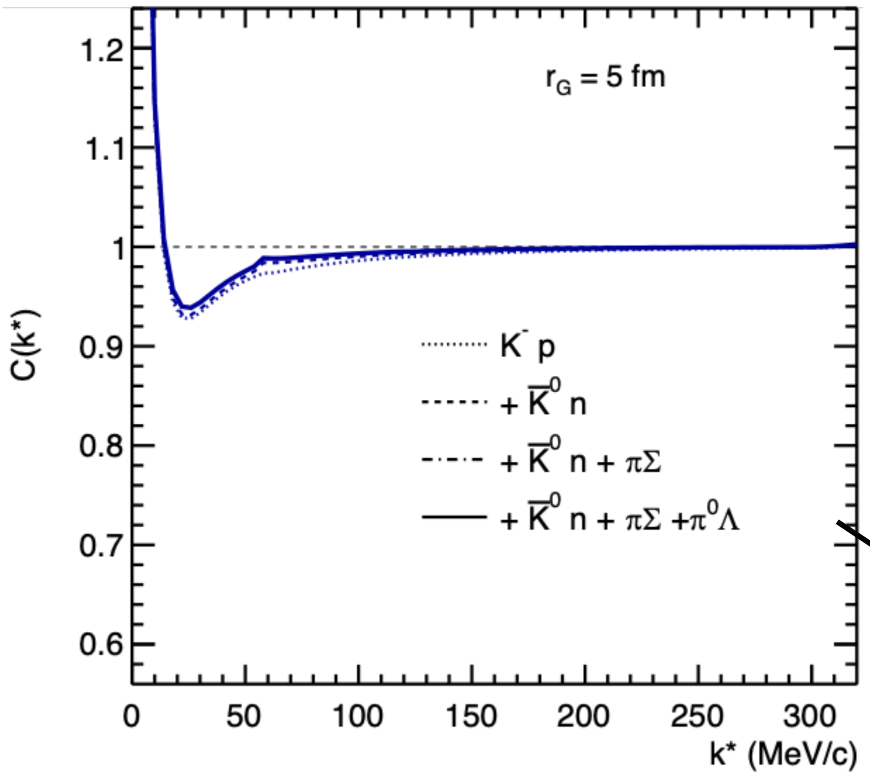

- Inelastic contributions negligible as the source size increases

$$C_{A-B}(k^*) = \int S(r)\ |\psi_{1\to1}(k^*, r)|^2\, d^3r + \sum_{j\neq1} w_j^{prod} \int S_j(r)\ \left|\psi_{j\to1}(k_j^*, r)\right|^2 d^3r = \mathcal{N}(k^*)\frac{N_{same}(k^*)}{N_{mixed}(k^*)}$$

elastic
A-B → A-B

inelastic
C-D → A-B, …

J. Haidenbauer Nucl.Phys.A 981 (2019)
Y. Kamiya et al. Phys.Rev.Lett. 124 (2020)
V.M.S., L. Fabbietti, O. Vazquez-Doce 2012.09806

Small vs large colliding systems

- At ALICE by changing the colliding system we can probe distances ranging from 1 fm up to 10 fm

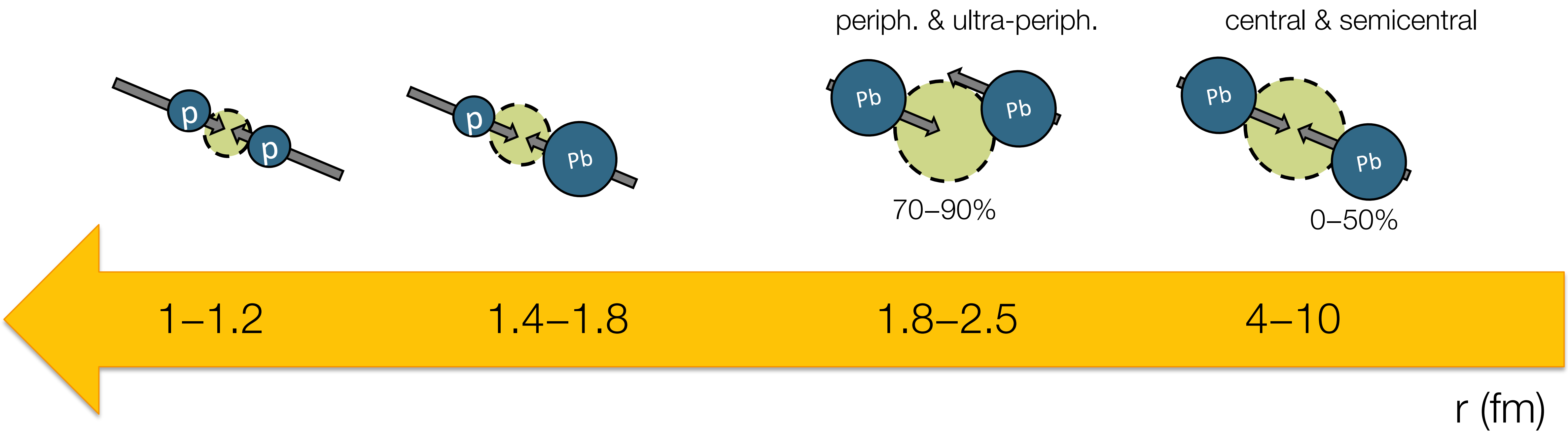

K^--p and K^+-p in pp 5,7,13 TeV, p–Pb and Pb–Pb 70–90% 5.02 TeV

p–$\overline{\mathrm{p}}$,p-$\overline{\Lambda}$ and Λ-$\overline{\Lambda}$ in pp HM 13 TeV and Pb–Pb 5.02 TeV

K^--p and K^+-p femtoscopy

K⁻-p femtoscopy: the antikaon-nucleon interaction

Λ(1405) molecular state

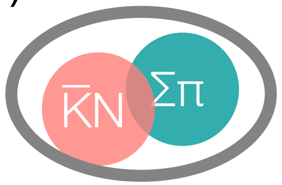

Λ(1405)→Σπ

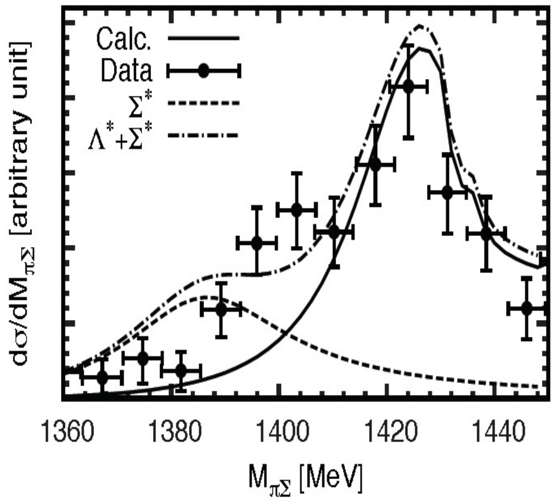

Kaonic hydrogen

SIDDHARTA Coll. PLB 704 (2011)

Scattering Experiments

Ikeda et al. Nucl.Phys.A 881 (2012)

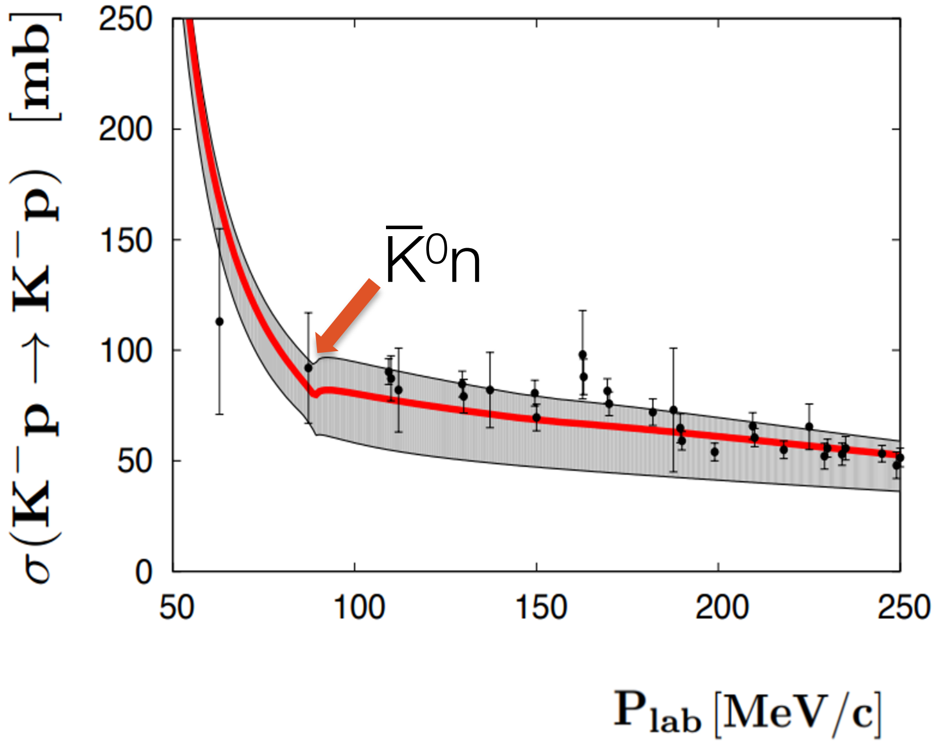

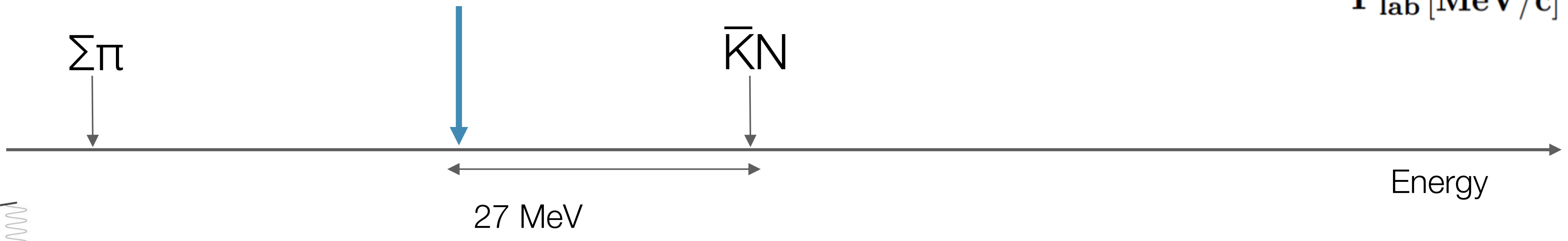

K⁻-p femtoscopy: the antiKaon-nucleon interaction

Λ(1405) molecular state

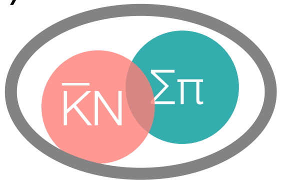

Λ(1405)→Σπ

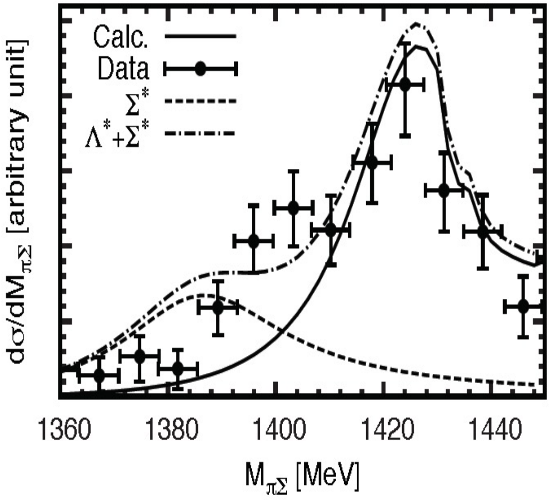

Scattering Experiments

Ikeda et al. Nucl.Phys.A 881 (2012)

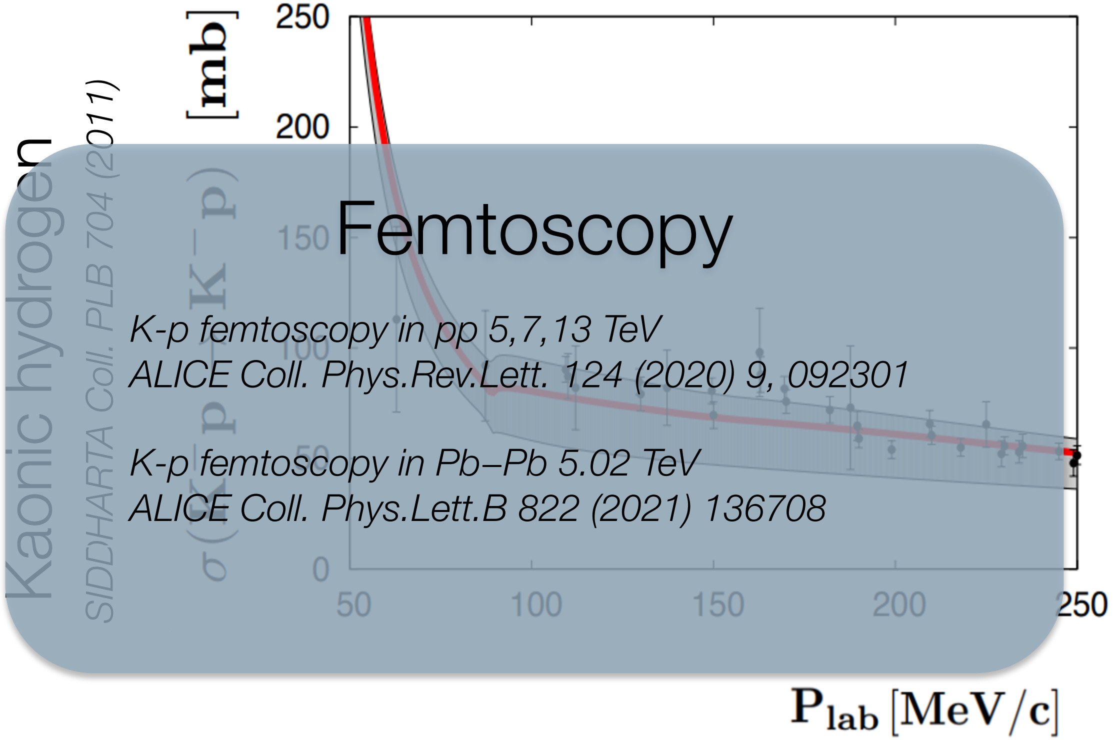

Femtoscopy

K-p femtoscopy in pp 5,7,13 TeV
ALICE Coll. Phys.Rev.Lett. 124 (2020) 9, 092301

K-p femtoscopy in Pb–Pb 5.02 TeV
ALICE Coll. Phys.Lett.B 822 (2021) 136708

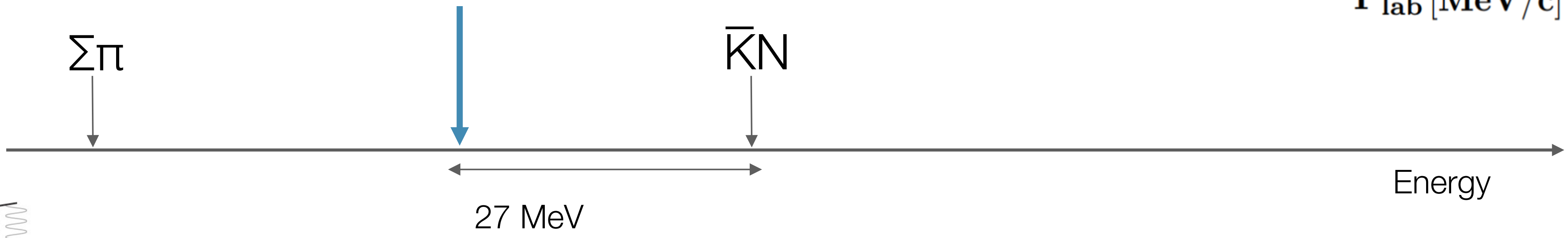

K⁻–p femtoscopy: smallest and largest colliding systems

$$C(k^*) = \int S(r)\, |\psi_{1\to1}(k^*, r)|^2 d^3r + \sum_{j=\Sigma\pi,\bar{K}^0 n} w_j^{prod} \int S_j(r)\, |\psi_{j\to1}(k_j^*, r)|^2 d^3r$$

χEFT Kyoto model:
Ikeda et al. NPA 881 (2012), PLB706 (2011)
Kamiya et al. PRL 124 (2020)
Mihayara et al. PRC95 (2017)

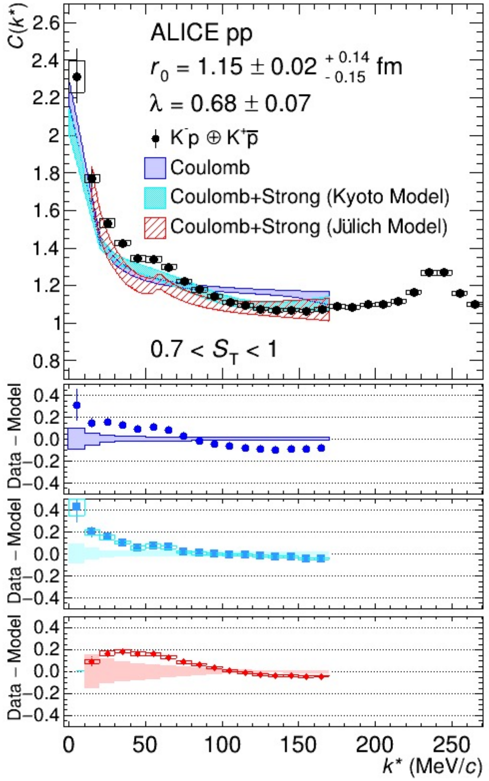

ALICE Coll. Phys.Rev.Lett. 124 (2020) 9, 092301

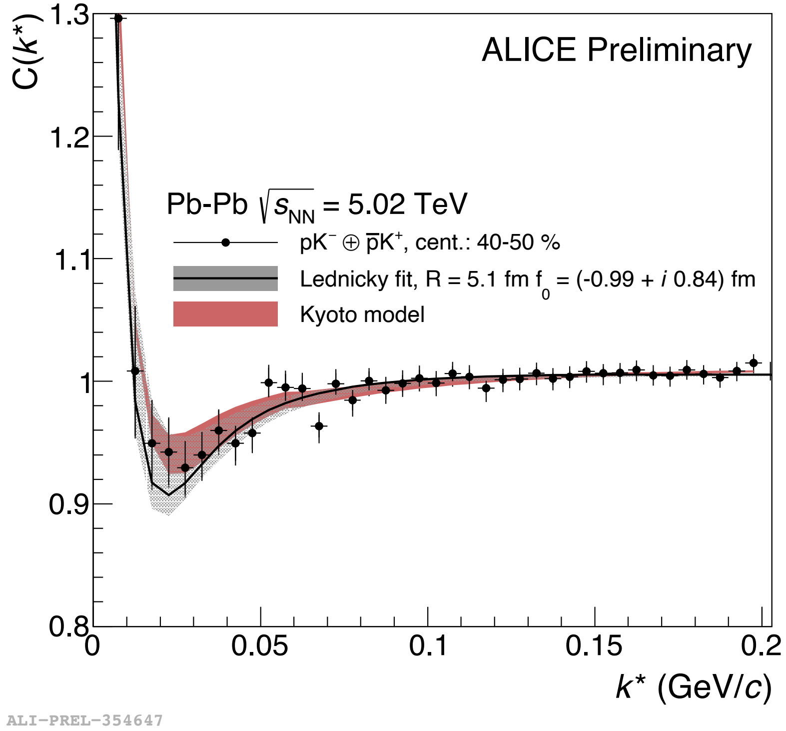

ALICE Coll. Phys.Lett.B 822 (2021) 136708

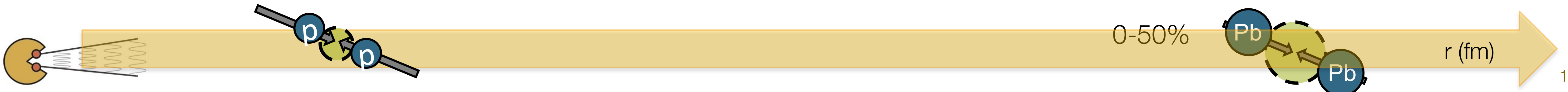

The conversion weights in K^-–p femtoscopy

- Modification of the conversion weights leads to a better agreement with the data
  - *see Phys.Rev.Lett. 124 (2020) 13, 132501*
- Conversion weights extracted from kinematics and thermal model predictions in pp, p-Pb and Pb-Pb
  - still agreement data/model?
  - provide constraints for the $\overline{K}^0$n coupling
- Perform the measurements in peripheral p-Pb and Pb-Pb collisions → access intermediate source sizes

Y. Kamiya et al. Phys.Rev.Lett. 124 (2020) 13, 132501

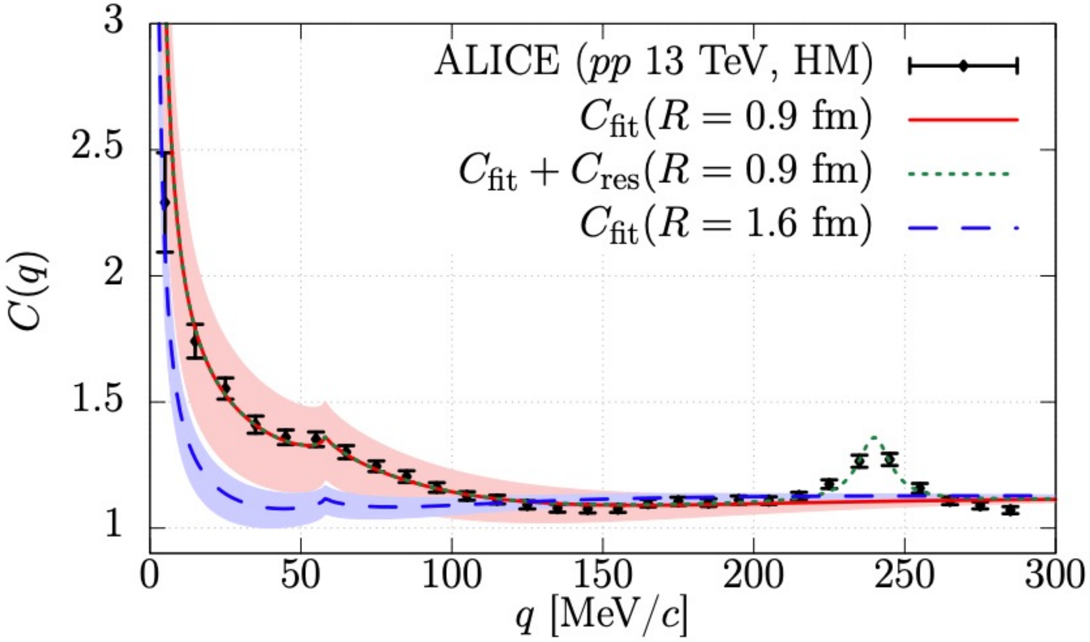

Paper in preparation
Dr. R. Lea
Dr. Y. Kamiya
Prof. Fabbietti
Prof A. Ohnishi
Prof. T.Hyodo
Maximilian Korweiser

K⁻–p femtoscopy in different colliding systems

Fixed from statistical model and Monte Carlo simulations with Blast-wave fits to data

$$C(k^*) = \int S(r)\,|\psi_{1\to1}(k^*, r)|^2\, d^3r + \sum_{j=\Sigma\pi,\bar{K}^0 n} w_j^{prod} \int S_j(r)\,|\psi_{j\to1}(k_j^*, r)|^2\, d^3r$$

χEFT Kyoto model:
Ikeda et al. NPA 881 (2012), PLB706 (2011)
Kamiya et al. PRL 124 (2020)
Mihayara et al. PRC95 (2017)

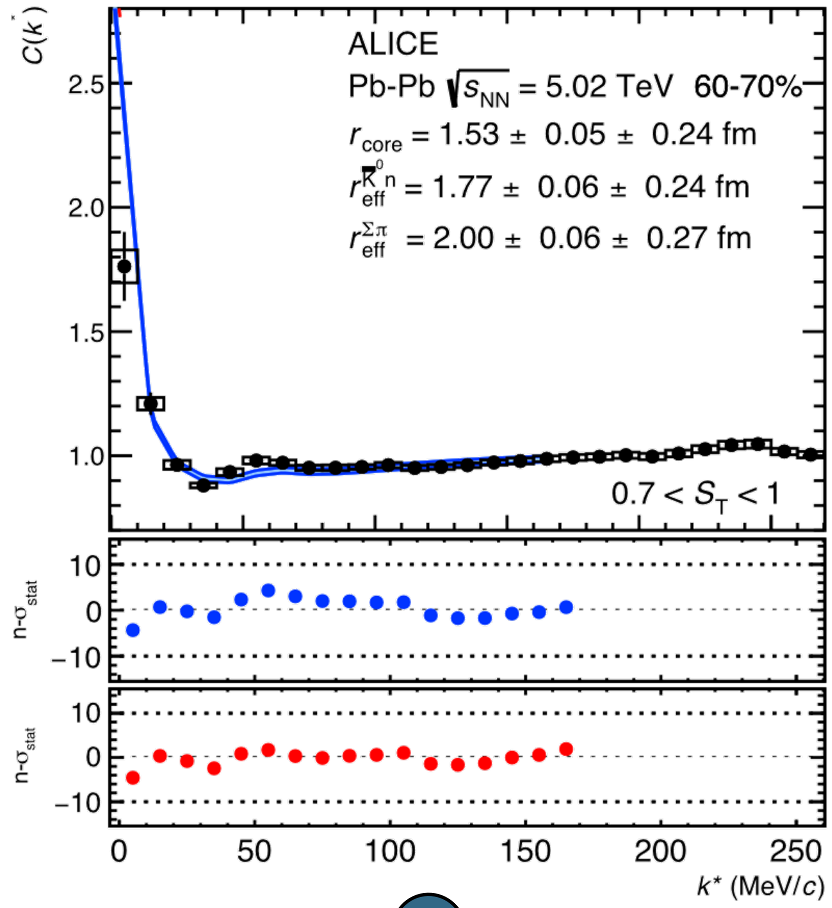

Paper in preparation

60-70%

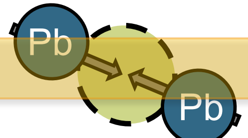

r (fm)

K⁻–p femtoscopy in different colliding systems

Fixed from statistical model and Monte Carlo simulations with Blast-wave fits to data

$$C(k^*) = \int S(r)\,|\psi_{1\to1}(k^*,r)|^2\,d^3r + \sum_{j=\Sigma\pi,\bar{K}^0n} w_j^{prod}\int S_j(r)\,|\psi_{j\to1}(k_j^*,r)|^2\,d^3r$$

χEFT Kyoto model:
Ikeda et al. NPA 881 (2012), PLB706 (2011)
Kamiya et al. PRL 124 (2020)
Mihayara et al. PRC95 (2017)

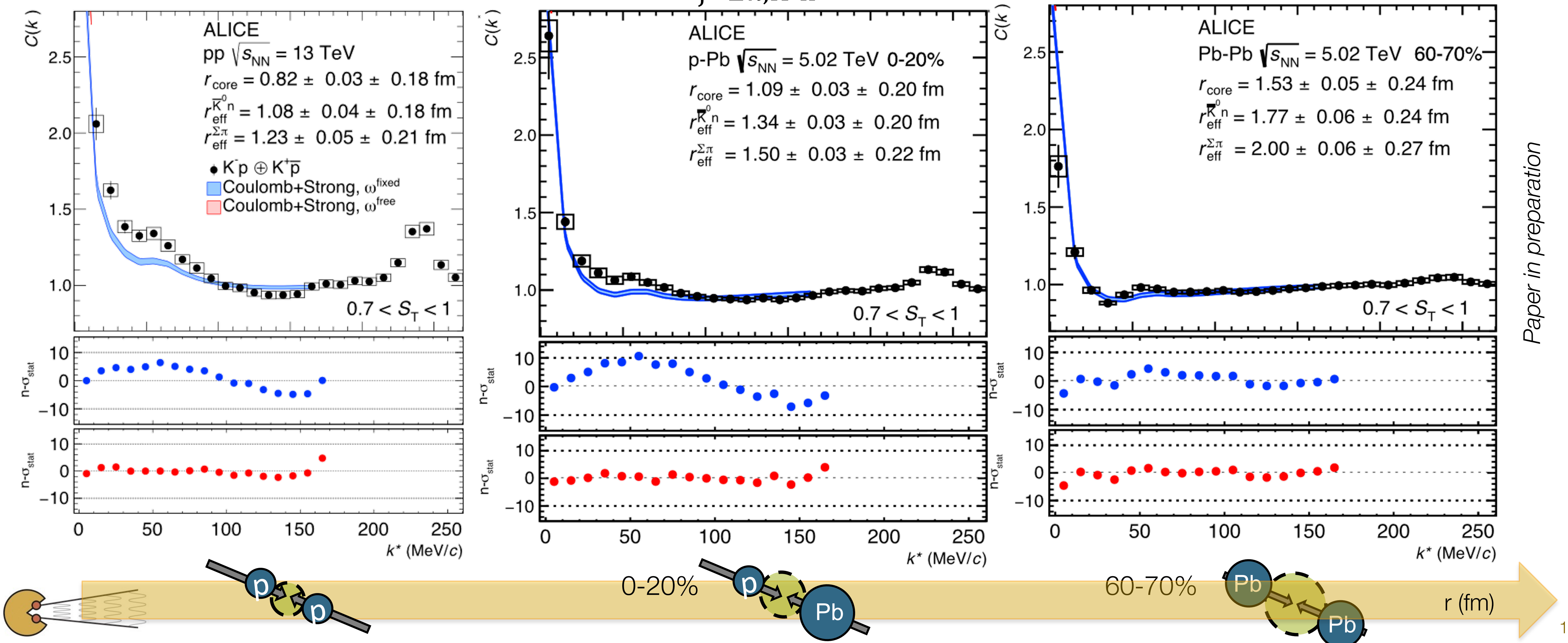

K⁻–p femtoscopy in different colliding systems

Fixed from statistical model and Monte Carlo simulations with Blast-wave fits to data

$$C(k^*) = \int S(r)\,|\psi_{1\to1}(k^*, r)|^2\, d^3r + \sum_{j=\Sigma\pi,\bar{K}^0 n} w_j^S \cdot w_j^{prod} \int S_j(r)\, |\psi_{j\to1}(k_j^*, r)|^2\, d^3r$$

χEFT Kyoto model:
Ikeda et al. NPA 881 (2012), PLB706 (2011)
Kamiya et al. PRL 124 (2020)
Mihayara et al. PRC95 (2017)

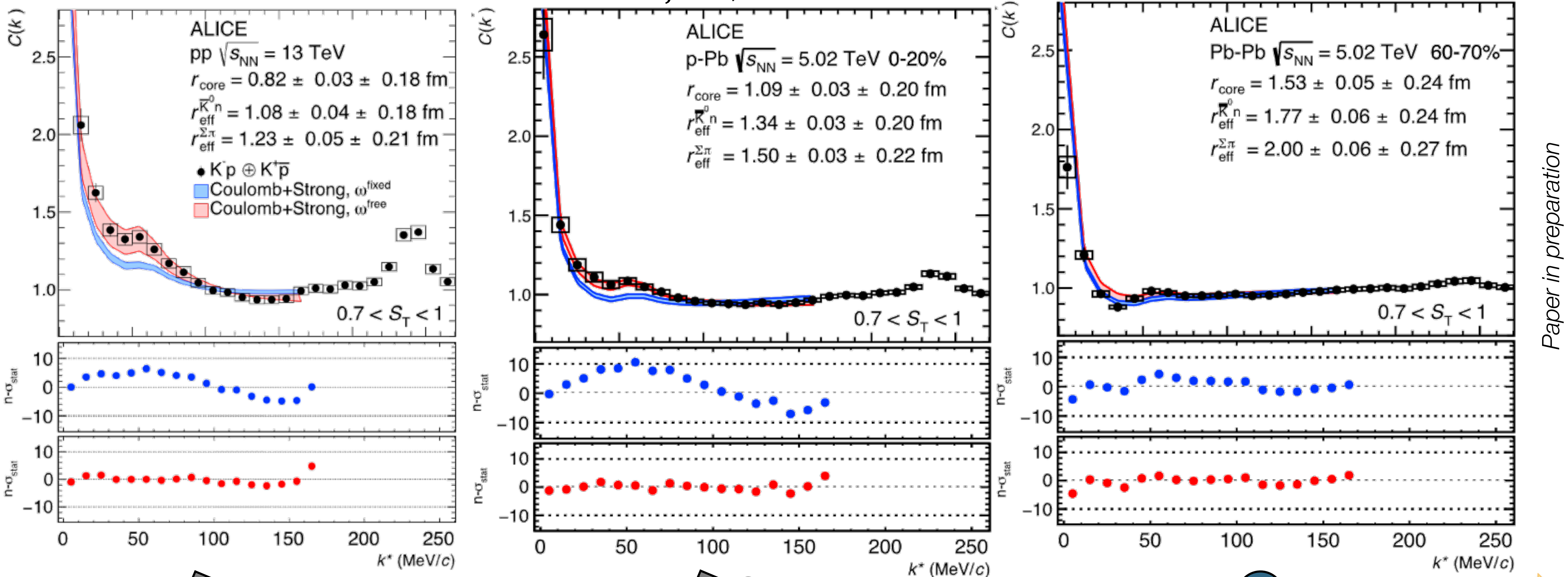

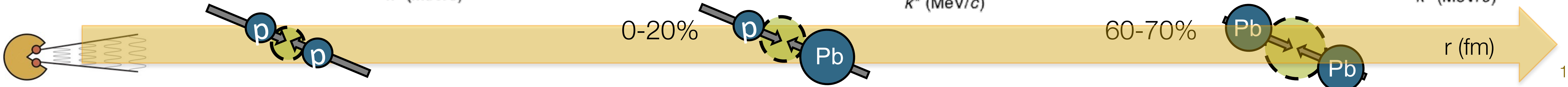

Extracted strong weights for Σπ and $\bar{K}^0$ n channels

Paper in preparation

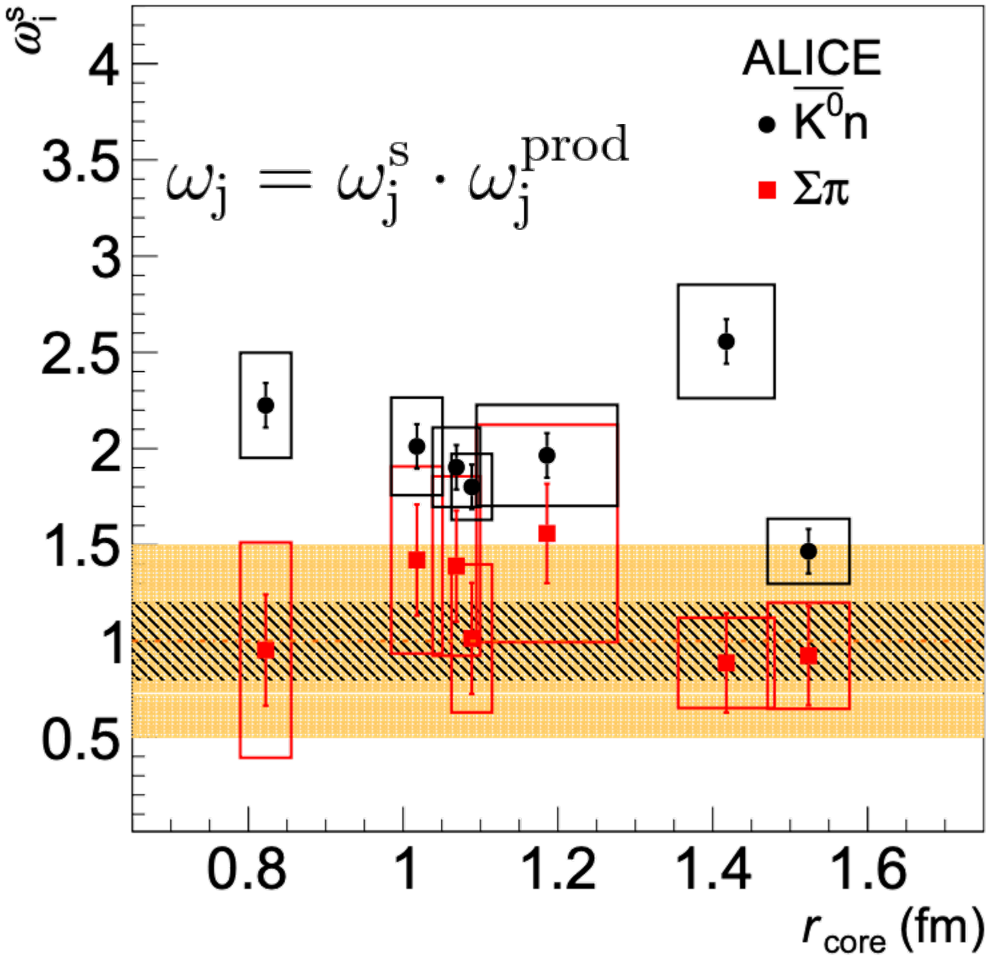

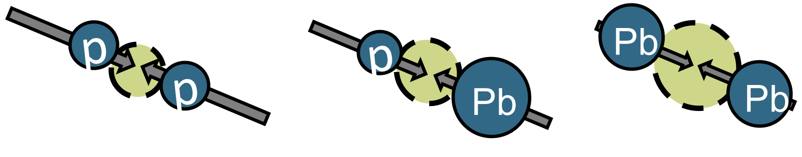

- deviation from unity for $\bar{K}^0$ n
- K^-p - $\bar{K}^0$ n too weak in chiral potentials
- Σπ consistent with unity

Baryon-antibaryon femtoscopy

The baryon-antibaryon interaction

Predictions for Baryonia??

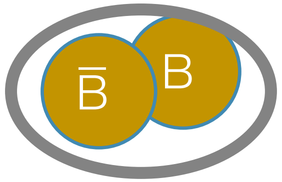

?

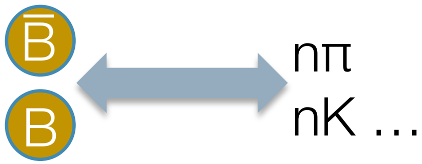

Annihilation dynamics
nπ,nK,πK,…

antiproton atoms

Scattering Experiments

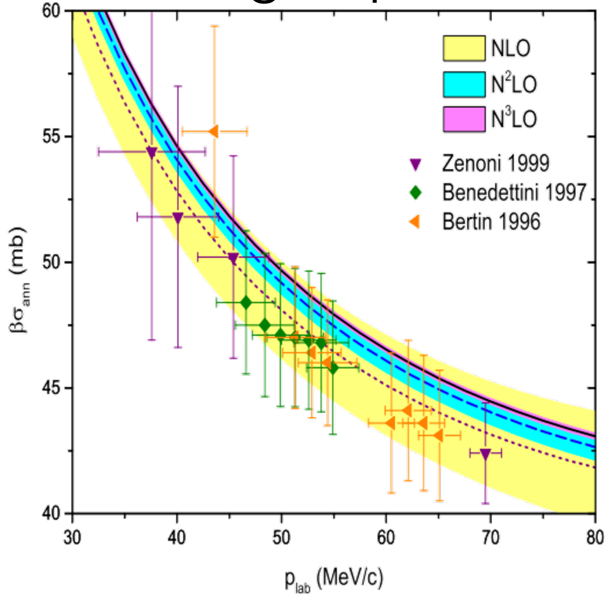

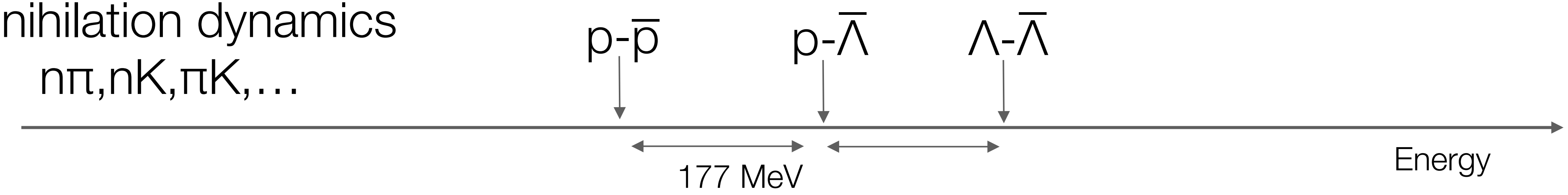

E. Klempt et al. Phys. Rept. 413 (2005)
E. Klempt et al. Phys. Rept. 368 (2002)
D. Zhou and R.G. E. Timmermans PRC86 (2012)
J. Haidenbauer et al. JHEP 1707 (2017)

The baryon-antibaryon interaction

Predictions for Baryonia??

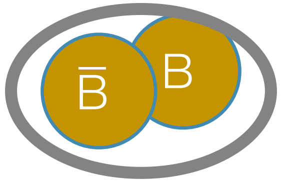

?

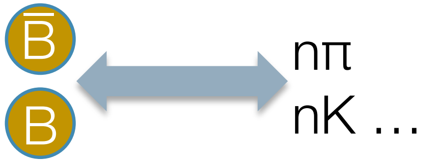

Annihilation dynamics
nπ,nK,πK,…

Scattering Experiments

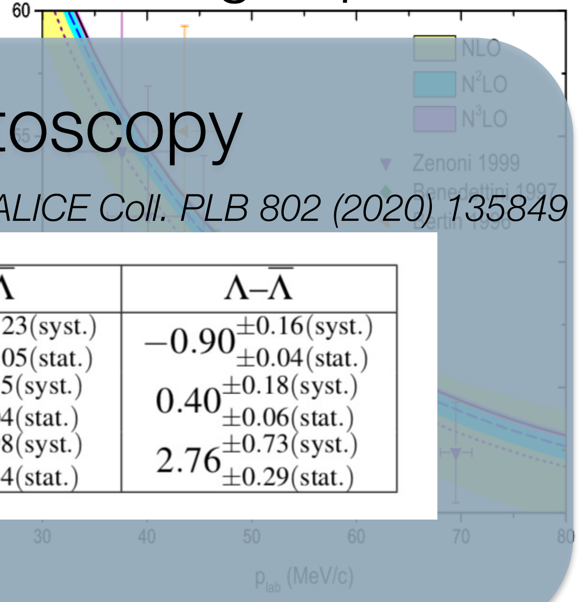

antiproton atoms

Femtoscopy

Pb-Pb 2.76 TeV results ALICE Coll. PLB 802 (2020) 135849

Parameter	p–$\overline{\Lambda}$	Λ–$\overline{\Lambda}$
$Re(f_0)$ (fm)	$-1.15^{\pm0.23(\mathrm{syst.})}_{\pm0.05(\mathrm{stat.})}$	$-0.90^{\pm0.16(\mathrm{syst.})}_{\pm0.04(\mathrm{stat.})}$
$Im(f_0)$ (fm)	$0.53^{\pm0.15(\mathrm{syst.})}_{\pm0.04(\mathrm{stat.})}$	$0.40^{\pm0.18(\mathrm{syst.})}_{\pm0.06(\mathrm{stat.})}$
d_0 (fm)	$3.06^{\pm0.98(\mathrm{syst.})}_{\pm0.14(\mathrm{stat.})}$	$2.76^{\pm0.73(\mathrm{syst.})}_{\pm0.29(\mathrm{stat.})}$

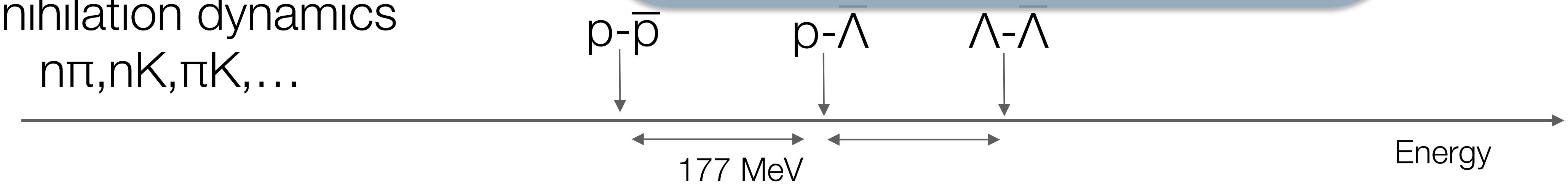

E. Klempt et al. Phys. Rept. 413 (2005)
E. Klempt et al. Phys. Rept. 368 (2002)
D. Zhou and R.G. E. Timmermans PRC86 (2012)
J. Haidenbauer et al. JHEP 1707 (2017)

Measured correlation for baryon-antibaryon in pp and Pb-Pb

ALICE Coll. arXiv: 2105.05190

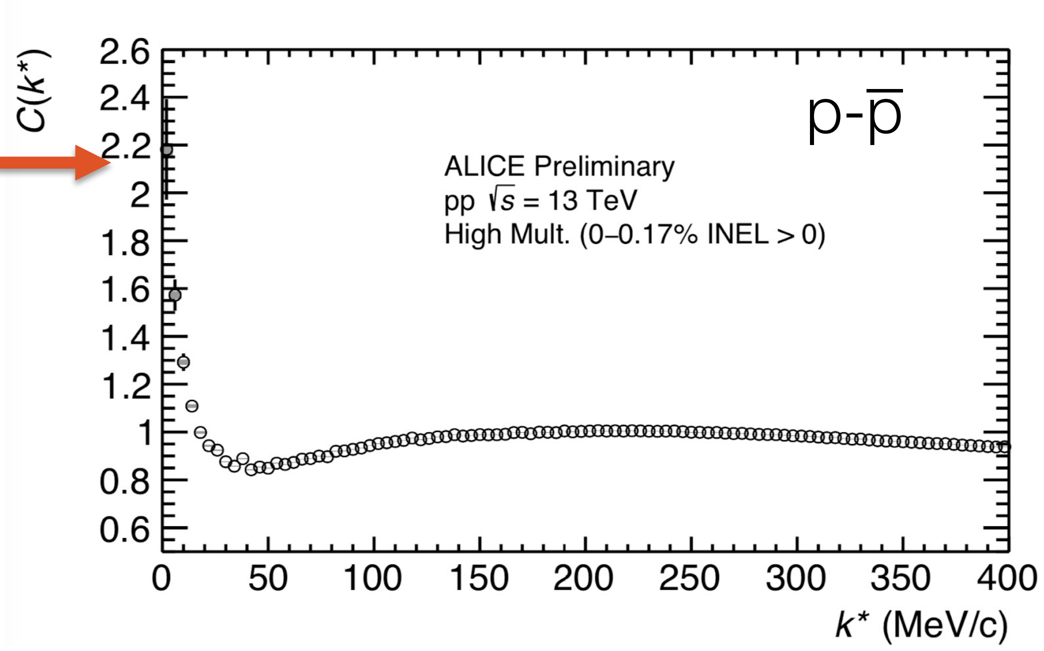

ALICE Coll. PLB 802 (2020) 135849

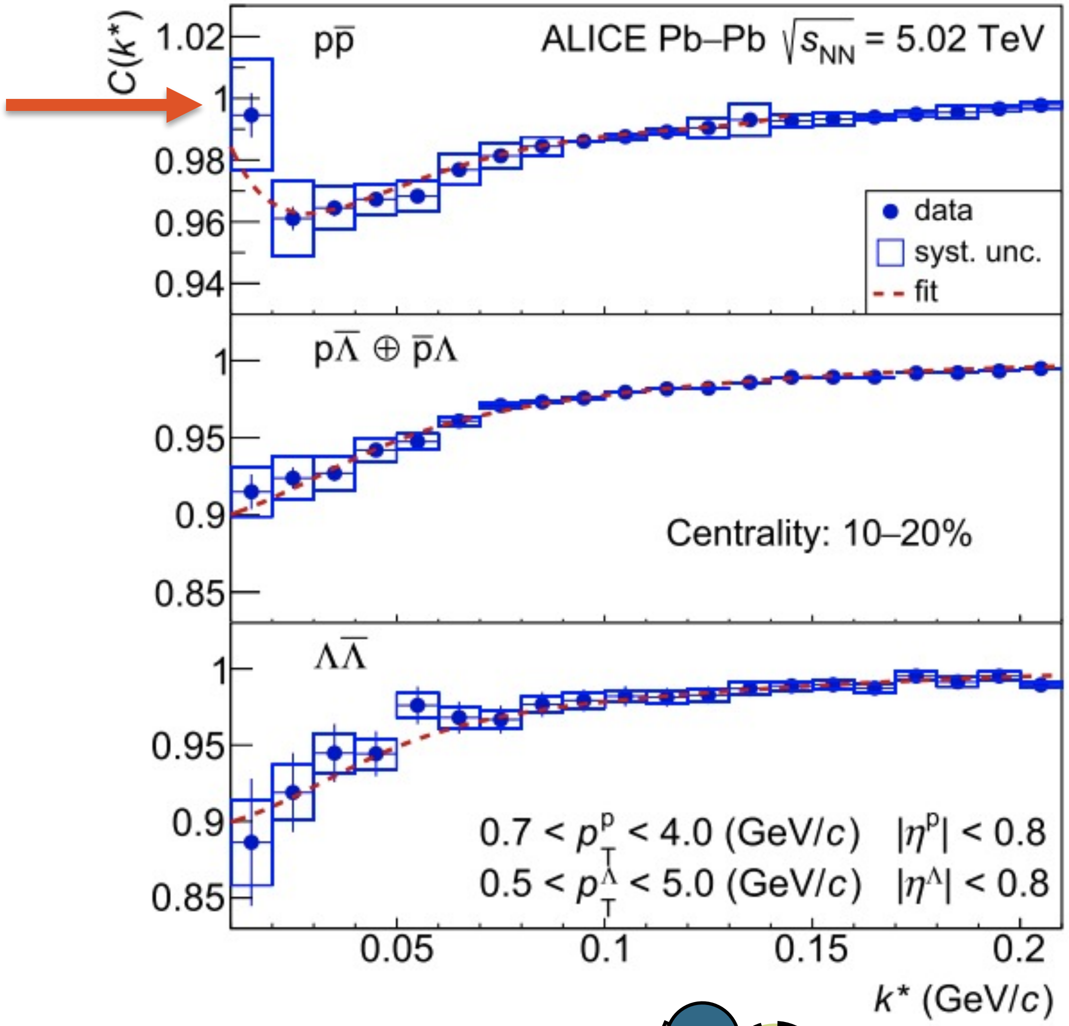

- Increase at low k*
  - Coulomb only?
  - feeding from annihilation channels?

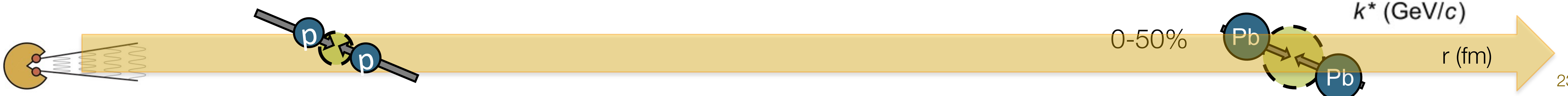

Measured correlation for baryon-antibaryon in pp and Pb-Pb

ALICE Coll. arXiv: 2105.05190

ALICE Coll. PLB 802 (2020) 135849

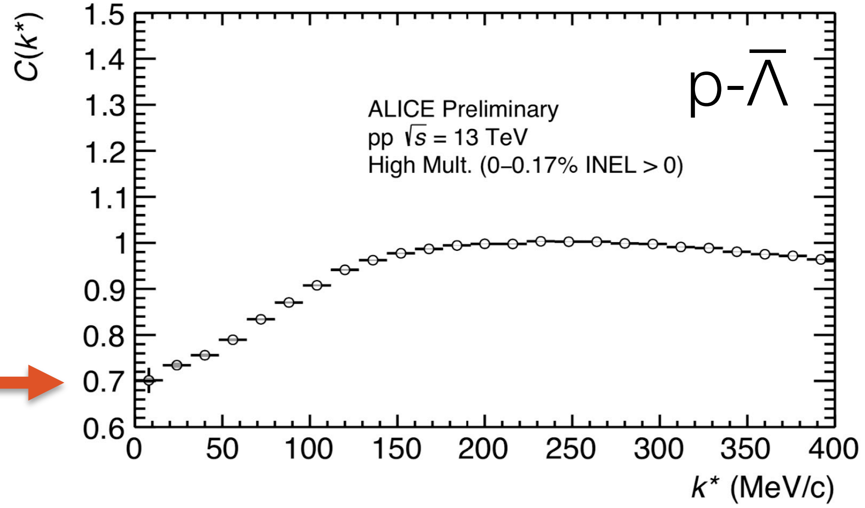

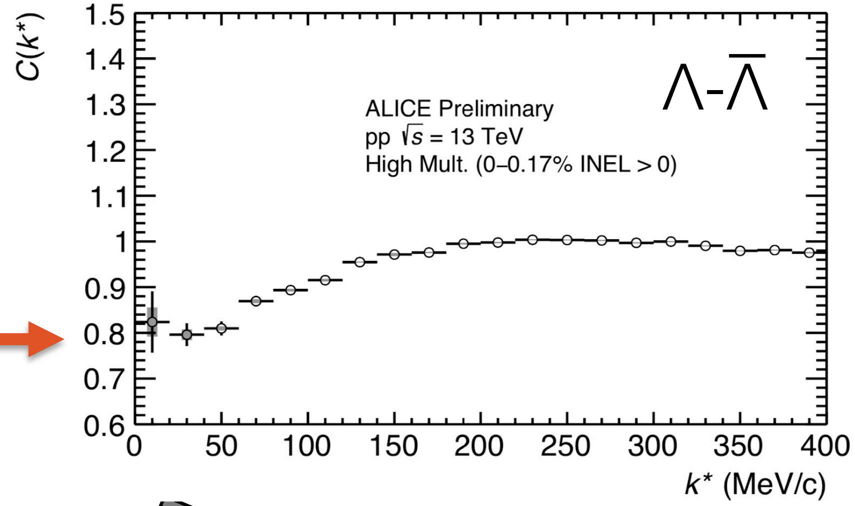

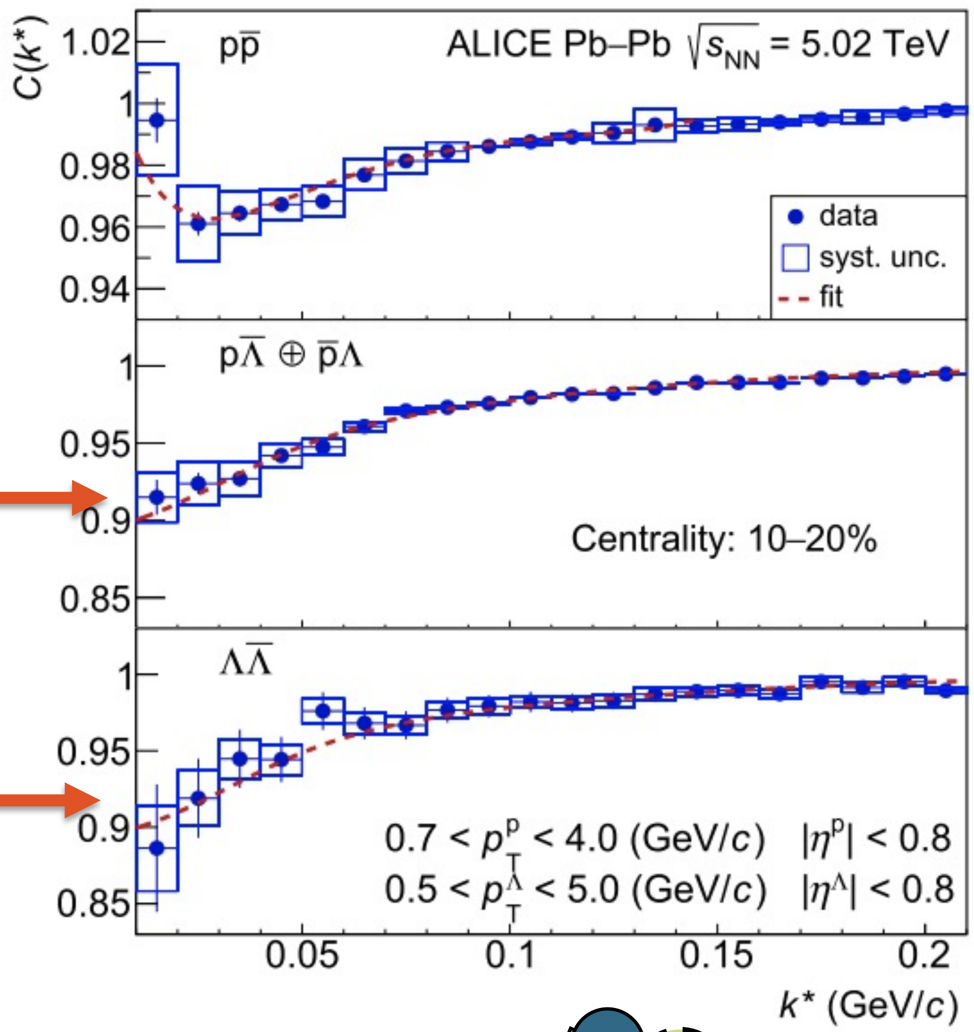

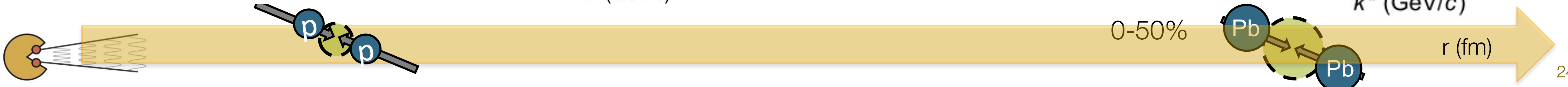

Results on p-$\bar{p}$: modeling the correlation

ALICE

elastic   n-$\bar{n}$ → p-$\bar{p}$

$$C_{p-\bar{p}}(k^*) = \int S(r)|\psi_{p\bar{p}\to p\bar{p}}|^2 d^3r + \int S(r)|\psi_{n\bar{n}\to p\bar{p}}|^2 d^3r$$

- Chiral Effective Field Theory at N^{3}LO (with n-$\bar{n}$ coupled-channel) wavefunctions with Coulomb
  - S and P waves, tuned to scattering data and protonium

J. Haidenbauer et al. JHEP 1707 (2017)
D.Mihailov et al. Eur.Phys.J.C 78 (2018) 5, 394
Haidenbauer et al.,PRD 92 (2015) 5, 054032

Results on p-$\bar{p}$: modeling the correlation

elastic | n-$\bar{n}$ → p-$\bar{p}$ | multi-meson annihilation channels

$$C_{p-\bar{p}}(k^*) = \int S(r)|\psi_{p\bar{p}\to p\bar{p}}|^2 d^3r + \int S(r)|\psi_{n\bar{n}\to p\bar{p}}|^2 d^3r + \sum_{PW} \rho_{PW}\,\omega_{PW} \int S(r)|\psi^{PW}_{p\bar{p}\to p\bar{p}}|^2 d^3r$$

- Chiral Effective Field Theory at N^{3}LO (with n-$\bar{n}$ coupled-channel) wavefunctions with Coulomb
  - S and P waves, tuned to scattering data and protonium

- Approximate inclusion of annihilation channels (X→ p-$\bar{p}$) using the Migdal-Watson approximation
  - elastic WF rescaled by a coupling weight ω_{PW} to be fitted to data
  - Investigation on the shape of each PWs to reduce number of parameters
    - $^1S_0$ for S states
    - $^3P_0$ and $^1P_1$ for P states

- Calculations performed with CATS framework

J. Haidenbauer et al. JHEP 1707 (2017)
D.Mihailov et al. Eur.Phys.J.C 78 (2018) 5, 394
Haidenbauer et al.,PRD 92 (2015) 5, 054032

Results on p-$\bar{p}$: modeling the correlation

- No cusp of n-$\bar{n}$ opening at k*~ 50 MeV/c → in agreement with charge-exchange cross-sections

- rise of CF at low k*
  - no agreement with Coulomb only
  - χEFT calculations with no explicit CC terms do not reproduce the data at low k*
  - evidence of annihilation channels feeding into p-$\bar{p}$ pairs

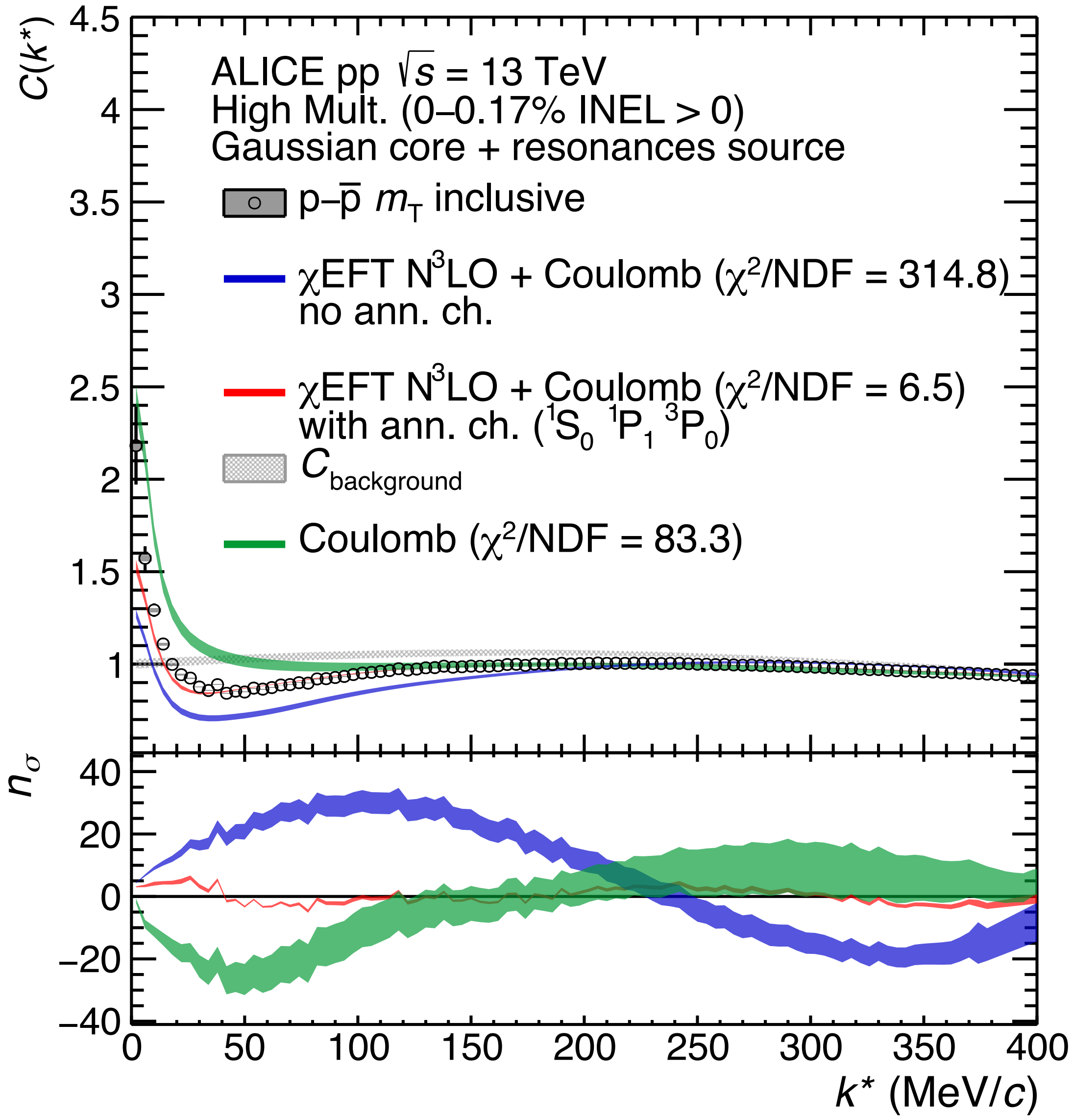

ALICE Coll. arXiv: 2105.05190

Correlation function for p-$\bar{p}$

- No cusp of n-$\bar{n}$ opening at k*~ 50 MeV/c → in agreement with charge-exchange cross-sections
- rise of CF at low k*
  - no agreement with Coulomb only
  - χEFT calculations with no explicit CC terms do not reproduce the data at low k*
  - evidence of annihilation channels feeding into p-$\bar{p}$ pairs
- **Annihilation channels X→ p-$\bar{p}$ included**
  - better agreement with the data is obtained
  - Dominant coupling weights in $^3P_0$ and $^1S_0$

ω_{3P0}= 40.04 ± 4.06 (stat) ± 4.24 (syst)

ω_{1S0}= 1.19 ± 0.10 (stat) ± 0.19 (syst)

PWA: D.Zhou and R.G. E. Timmermans PRC86 (2012)

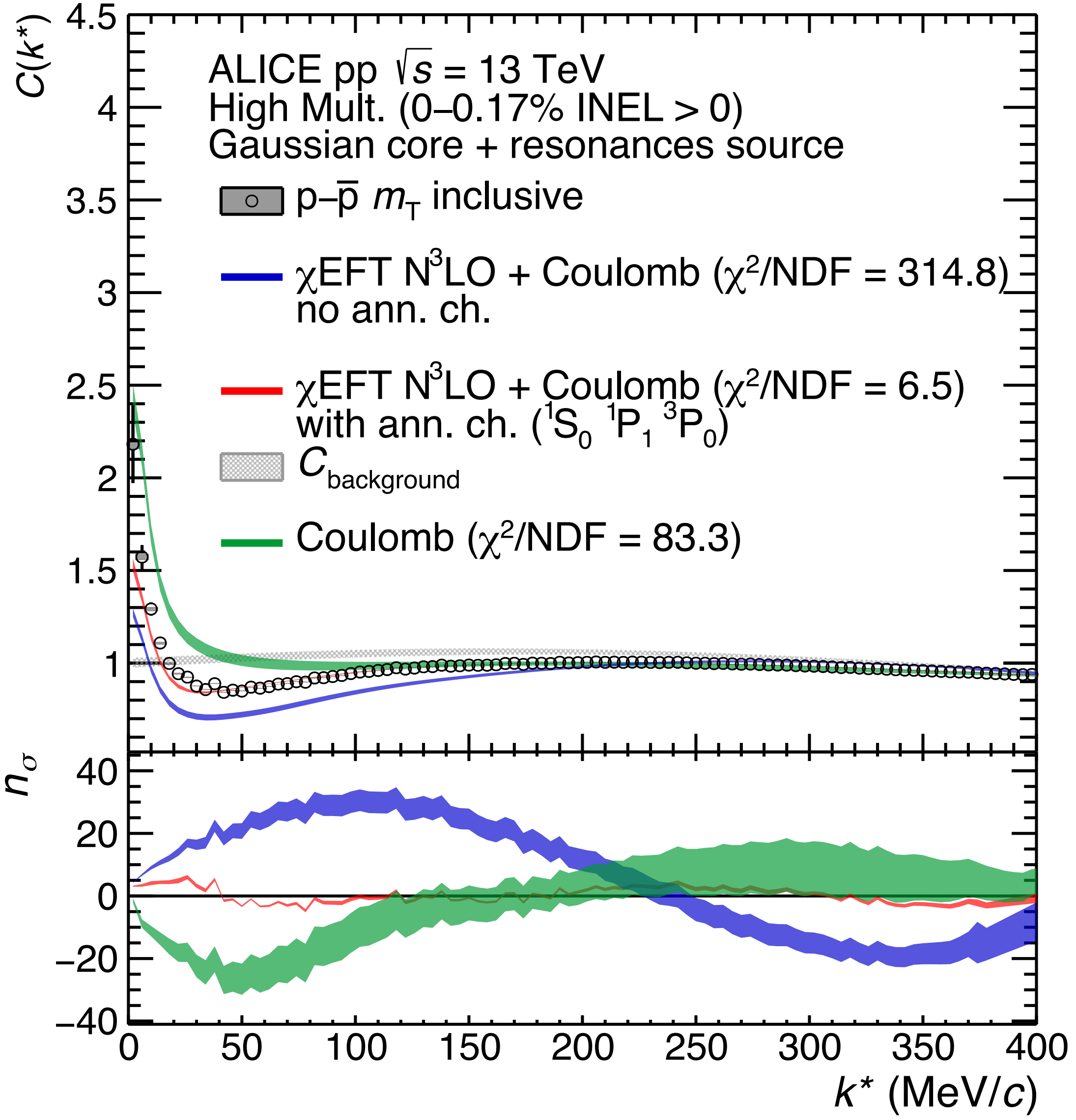

ALICE Coll. arXiv: 2105.05190

Results on Λ-$\bar{\Lambda}$ and p-$\bar{\Lambda}$ femtoscopy

- No exact wavefunctions available → single-channel Lednický-Lyuboshits formula (Re(f_0) , Im(f_0))
- Assuming the scattering parameters obtained in Pb–Pb
  - nice agreement with Λ-$\bar{\Lambda}$ data → inelastic part present but not dominant

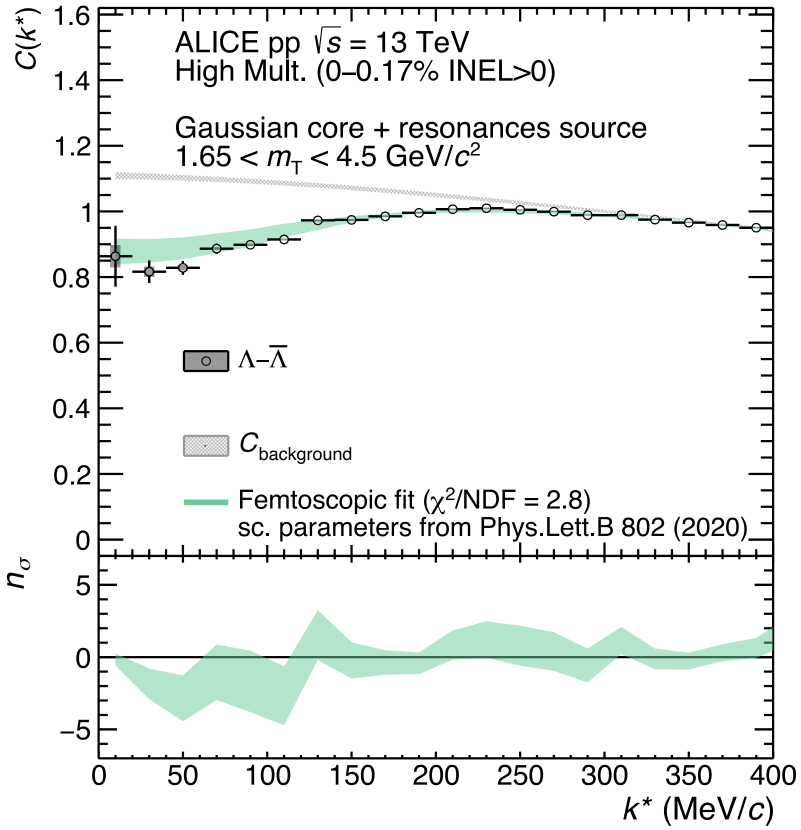

ALICE Coll. arXiv: 2105.05190

Results on Λ-$\bar{\Lambda}$ and p-$\bar{\Lambda}$ femtoscopy

- No exact wavefunctions available → single-channel Lednický-Lyuboshits formula
- Assuming the scattering parameters obtained in Pb–Pb
  - nice agreement with Λ-$\bar{\Lambda}$ data → inelastic part present but not dominant
  - underestimate of p-$\bar{\Lambda}$ data → large coupling to multi-meson annihilation channels

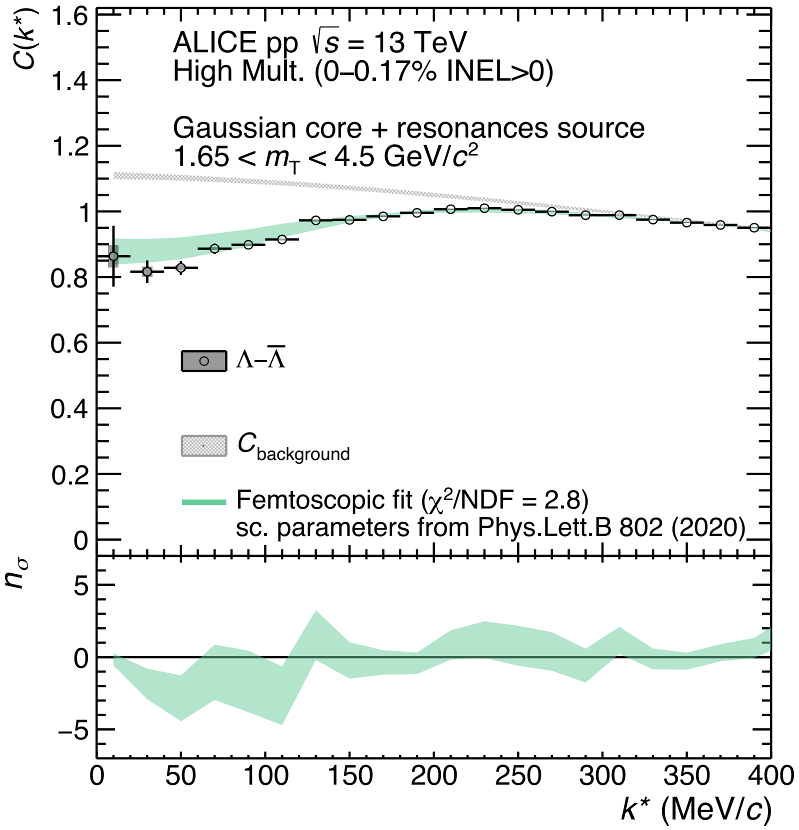

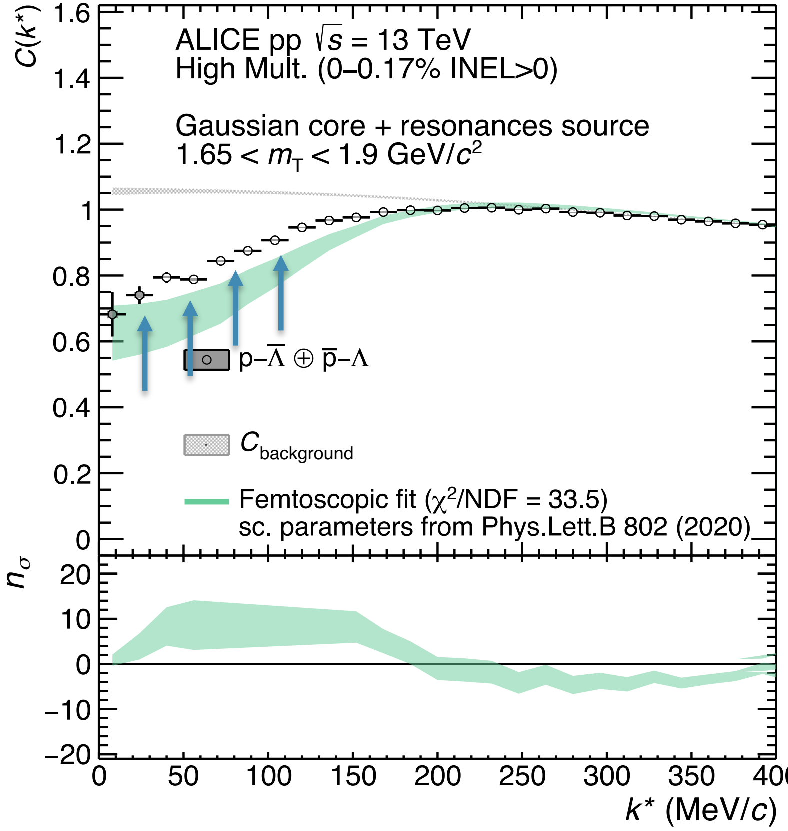

ALICE Coll. arXiv: 2105.05190

Results on Λ-$\bar{\Lambda}$ and p-$\bar{\Lambda}$ femtoscopy

- Elastic part Re(f_0) fixed from Pb–Pb data, free inelastic Im(f_0) and d_0
  - extracted values for Λ-$\bar{\Lambda}$ are compatible with Pb–Pb scattering parameters
  - to reproduce p-$\bar{\Lambda}$ data Im(f_0) has to increased by a factor ~ 5.3
- Larger presence of multi-meson annihilation channels in p-$\bar{\Lambda}$ → no bound states?

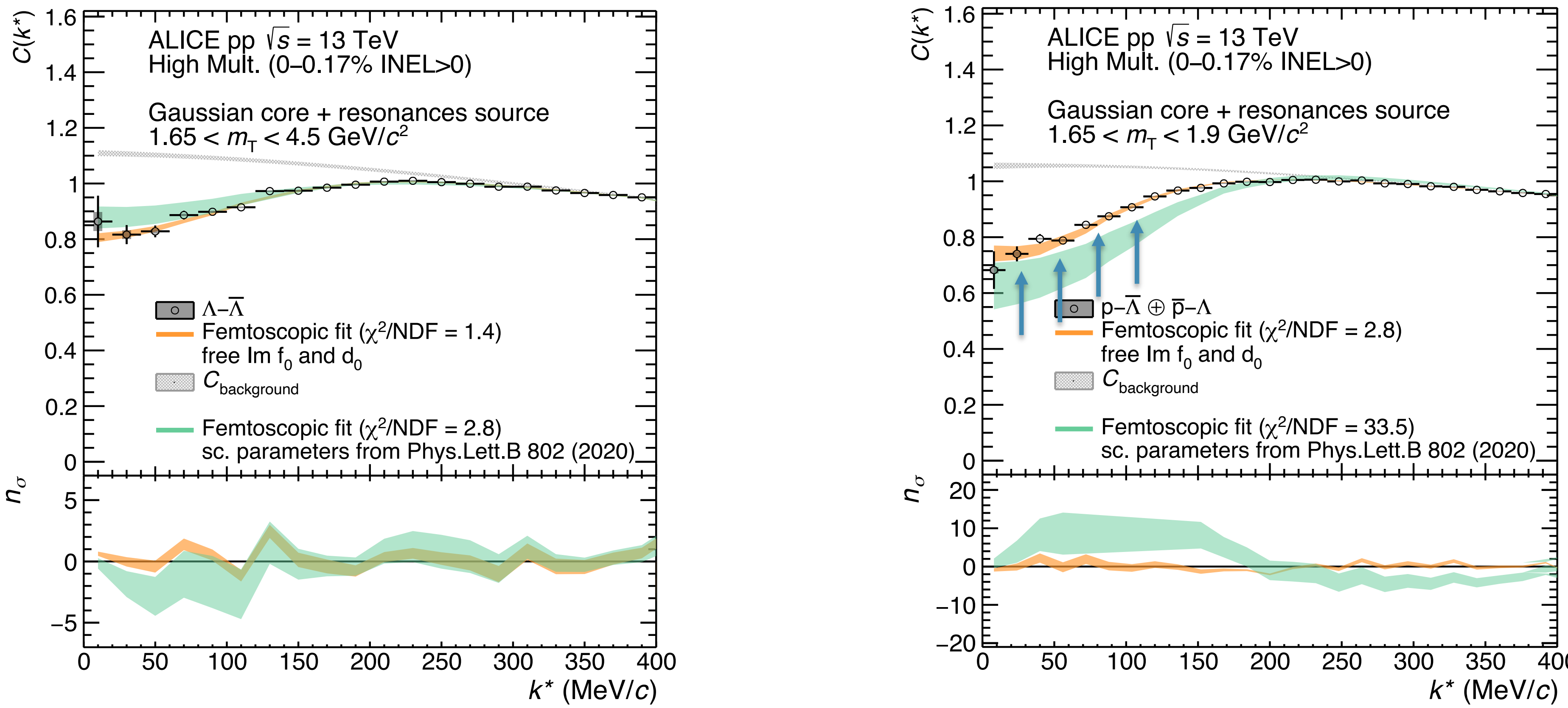

ALICE Coll. arXiv: 2105.05190

Results on Λ-$\bar{\Lambda}$ and p-$\bar{\Lambda}$ femtoscopy

- Estimates based on kinematics (EPOS) and SU(3) flavour symmetry for 2-meson channels (ππ,πK)
  - similar amount of p-$\bar{\Lambda}$ and Λ-$\bar{\Lambda}$ pairs at low k* (~6.4%)
  - coupling strength from meson-baryon SU(3) lagrangian for p-$\bar{\Lambda}$ ~ 3 times larger than Λ-$\bar{\Lambda}$

$$\frac{g_{2M\to p-\bar{\Lambda}} \times N_{2M\to p-\bar{\Lambda}}}{g_{2M\to \Lambda-\bar{\Lambda}} \times N_{2M\to \Lambda-\bar{\Lambda}}} \approx 6.3$$

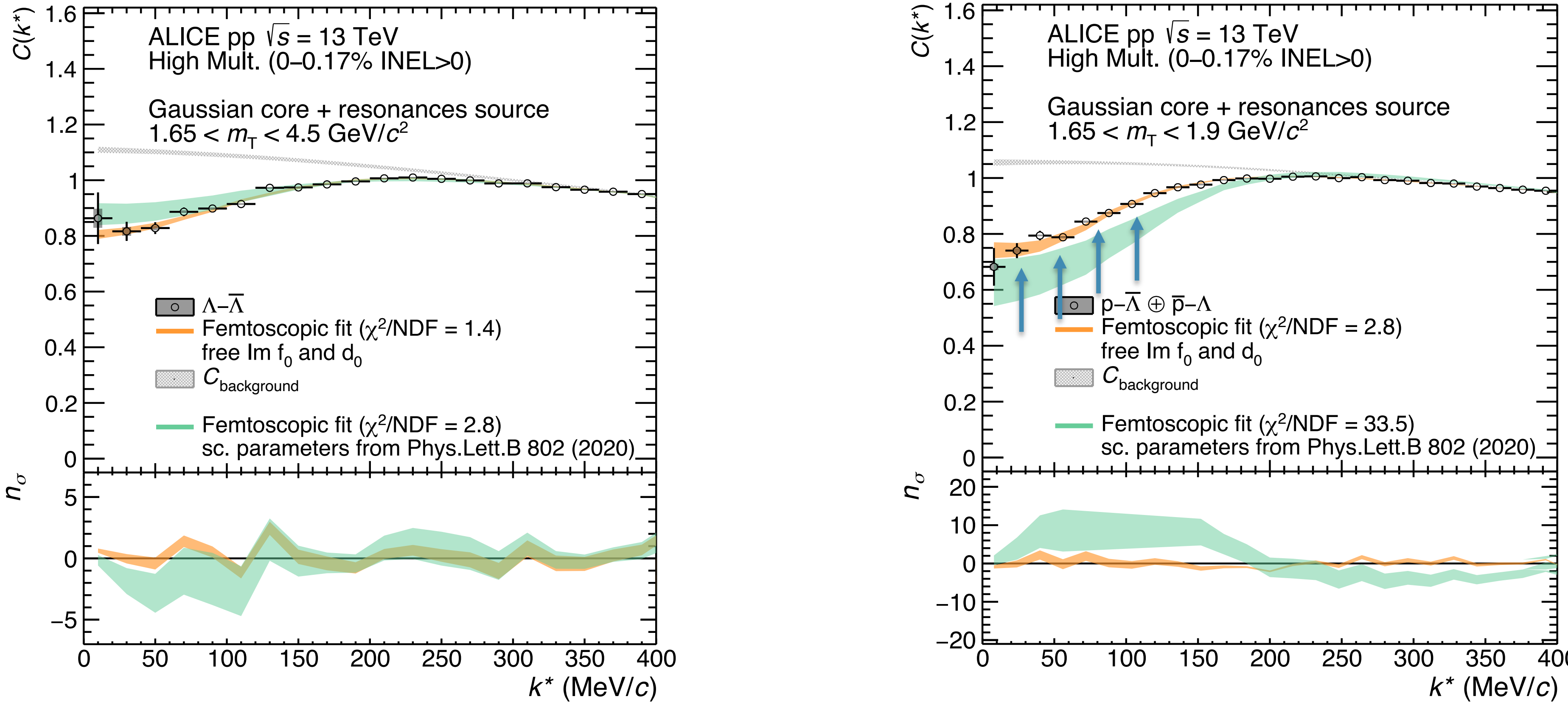

ALICE Coll. arXiv: 2105.05190

Conclusions

- Femtoscopy in small colliding systems
  - high-precision data at low momenta
  - sensitivity to inelastic channels as a function of the source size
- K^-–p in pp, peripheral p–Pb and ultra-per. Pb–Pb collisions
  - direct constraints on coupling to Σπ and $\overline{K}^0$ n
  - data suggests a stronger coupling to $\overline{K}^0$ n
- Baryon-antibaryon in pp collisions
  - Λ-$\overline{\Lambda}$ results annihilation not dominant and room for baryonia
  - p-$\overline{\Lambda}$ large presence of annihilation channels → no formation of bound states?
  - need for theoretical input on p-$\overline{\Lambda}$ and Λ-$\overline{\Lambda}$ interactions

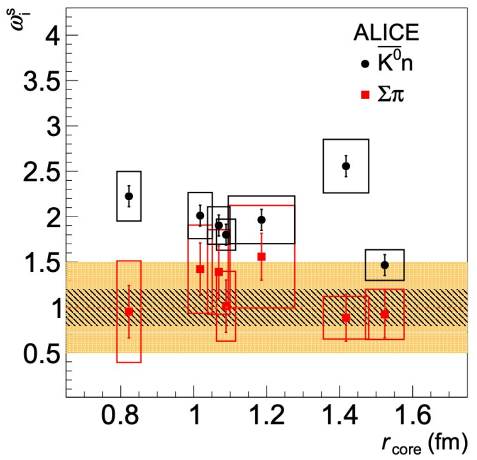

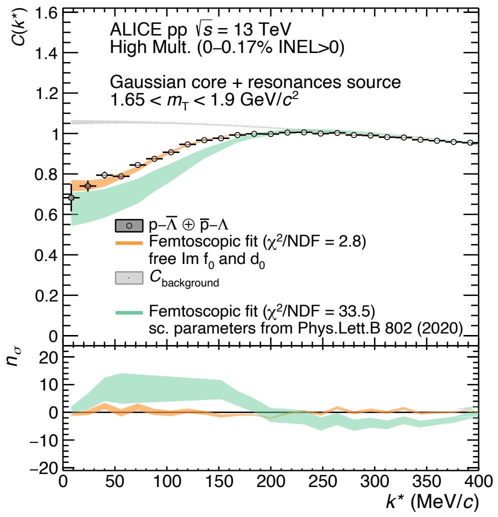

Run 1	*PRC 99 (2019) 024001*
Λ-Λ	*PLB 797 (2019) 134822*
p-Ξ	*PRL 123 (2019) 112002*
p-K in pp	*PRL 124 (2020) 09230*
p-Σ^0	*PLB 805 (2020) 135419*
source	*PLB 811 (2020) 135849*
p-Ω, p-Ξ	*Nature 588 (2020) 232-238*
p-Λ	*arXiv:2104.04427*
p-ϕ	*PRL 127 (2021) 172301*
p-K in Pb-Pb	*PLB 822 (2021) 136708*
B-antiB in pp	*arXiv:2105.05190*

more to come in the next months:
charm sector, 3-body correlations, p-d, Λ-Ξ,…

Additional slides

Basics of femtoscopy at LHC

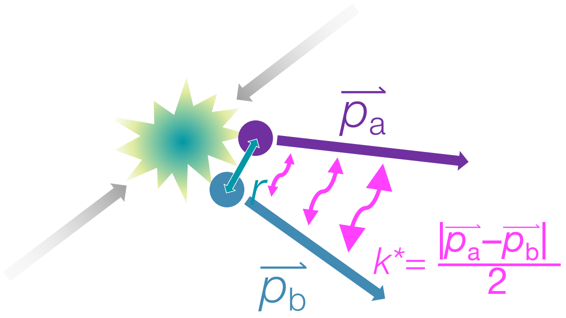

Emission source S(r*)

Interacting potential

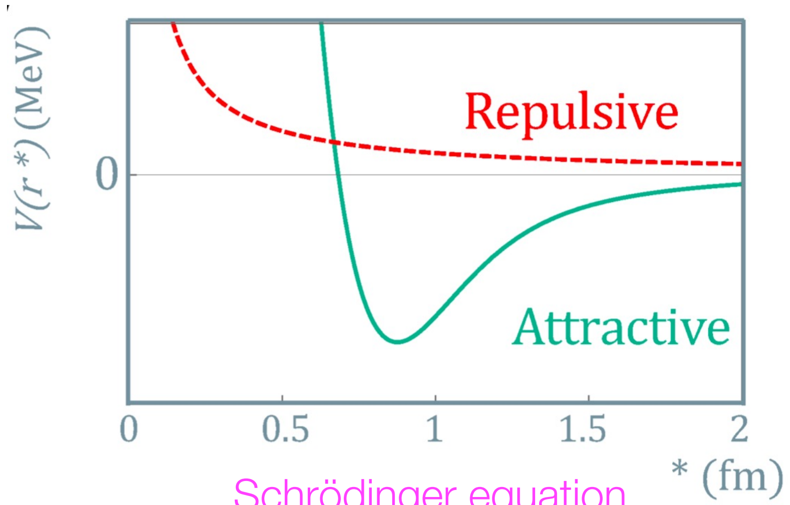

Schrödinger equation

Two-particle wave function

Correlation function

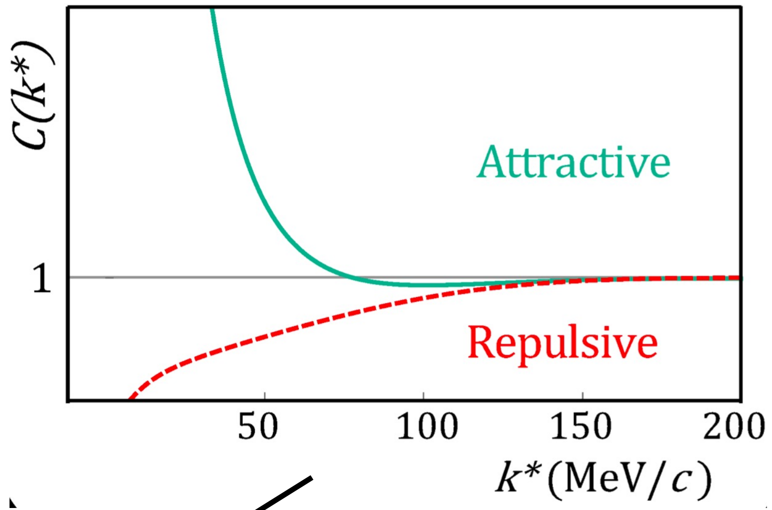

$$C(k^*) = \int S(\vec{r}^*)\left|\psi(\vec{k}^*,\vec{r}^*)\right|^2 d^3\vec{r}^* = \mathcal{N}(k*)\frac{N_{same}(k^*)}{N_{mixed}(k^*)}$$

CATS Framework: D. Mihaylov et al., Eur. Phys. J. C78 (2018) 394

Small Sources: Collective Effects and Strong Resonances

Fit with a 'core' Gaussian + Resonances

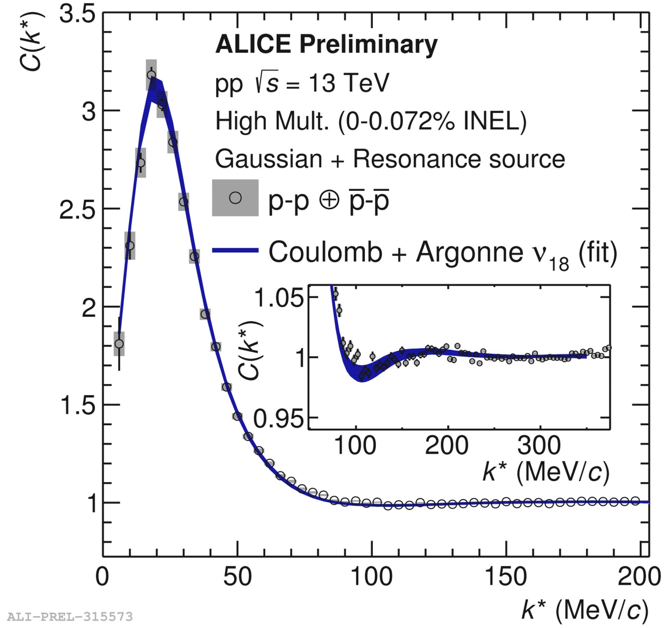

Core Radius

arXiv:2004.08018 accepted in PLB

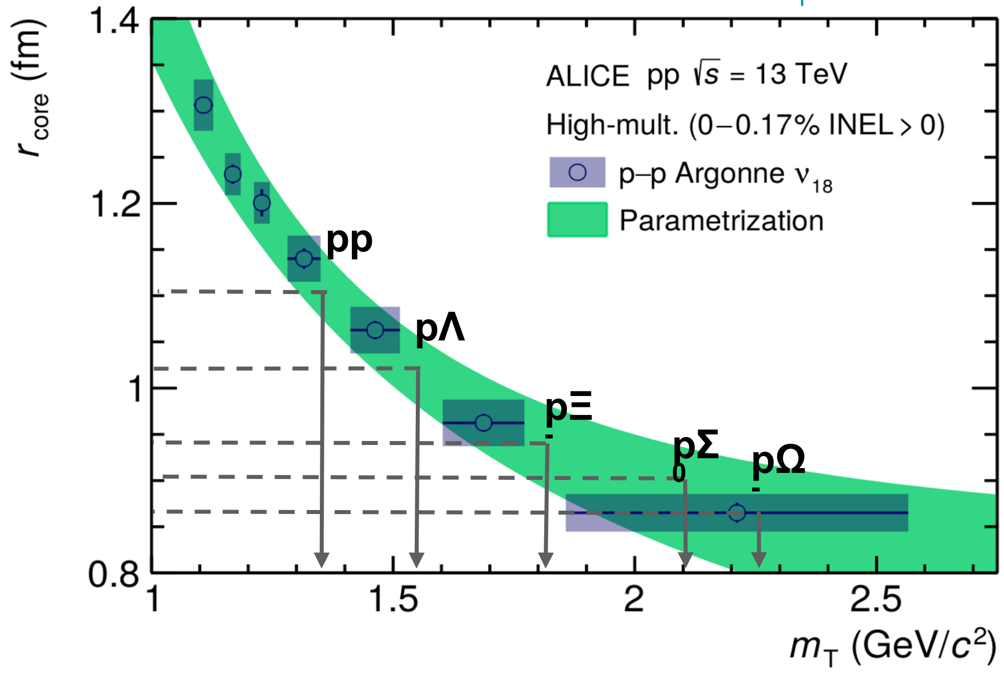

Effective Radius

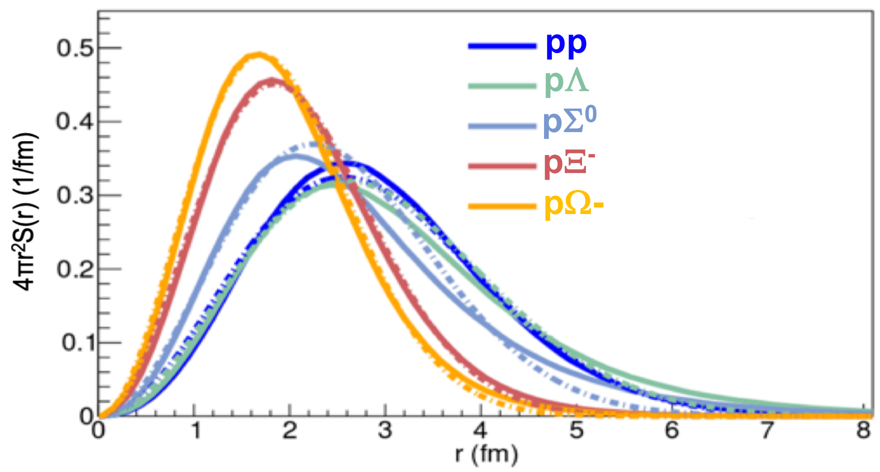

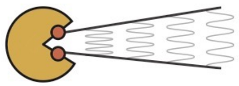

Pair	r_{Core} [fm]	r_{Eff} [fm]
pp	0.96	1.28
pΛ	0.88	1.3
pΣ^0	0.75	1.12
pΞ^-	0.8	0.92
pΩ-	0.73	0.85

K^-–p femtoscopy in pp and Pb-Pb collisions

- Disappearance of $\bar{K}^0$–n cusp at k*~ 60 MeV/*c* as the source increases
- χEFT Kyoto potential describes the data in all three systems
- Pb–Pb data well described by Lednicky single channel → negligible contribution from inelastic channels
- Pb–Pb results in agreement with scattering parameters from kaonic hydrogen

Ikeda et al. Nucl.Phys.A 881 (2012), PLB706 (2011)
Kamiya et al. PRL 124 (2020)
Mihayara et al. PRC95 (2017)

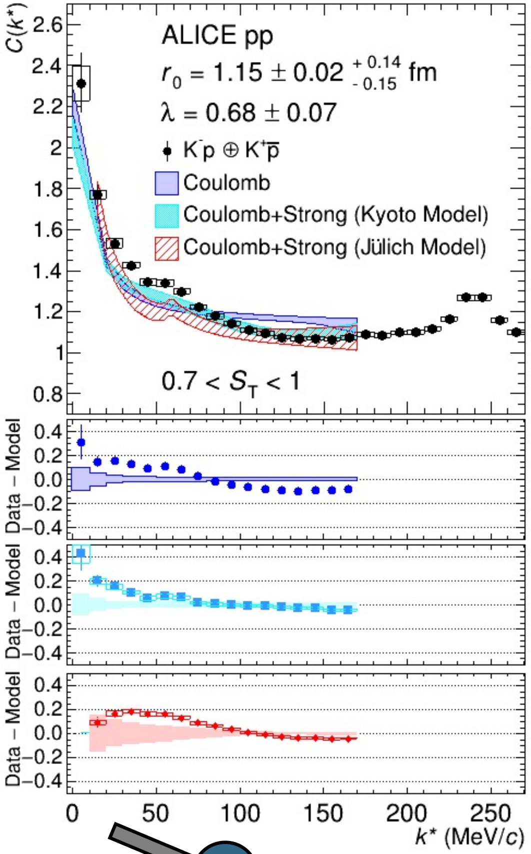

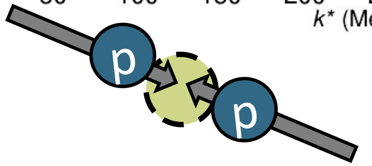

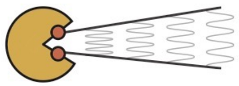

assuming w_j = 1

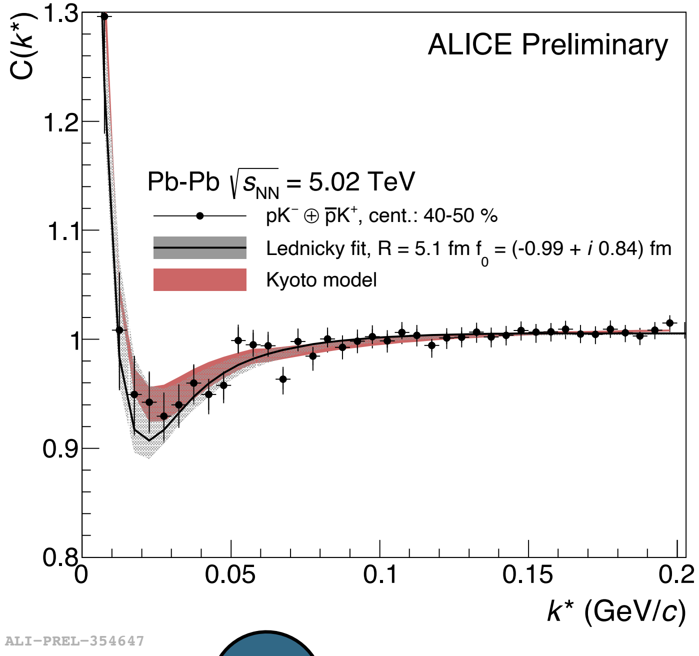

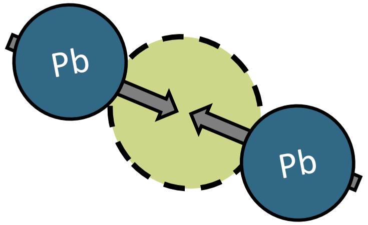

K⁺p correlations in pp

ALICE Coll. Phys.Rev.Lett. 124 (2020) 9, 092301

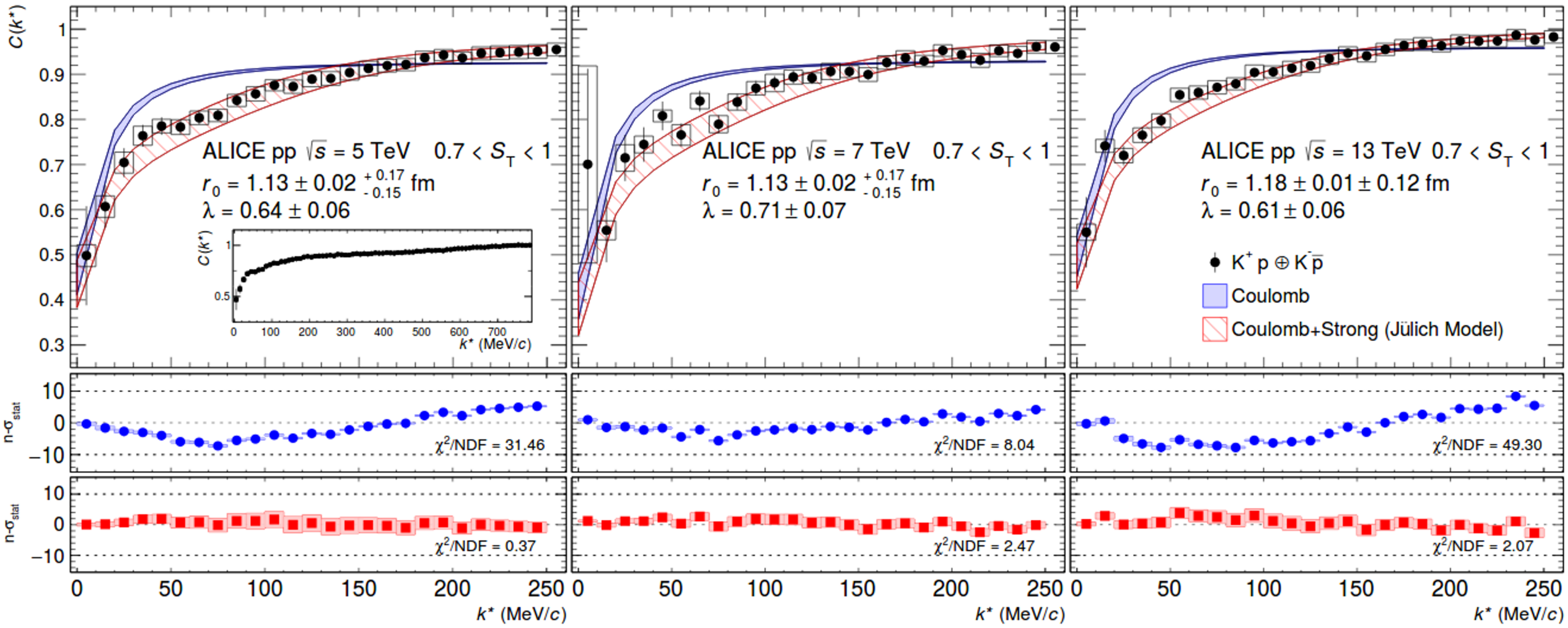

K^+p correlations in p–Pb and Pb–Pb

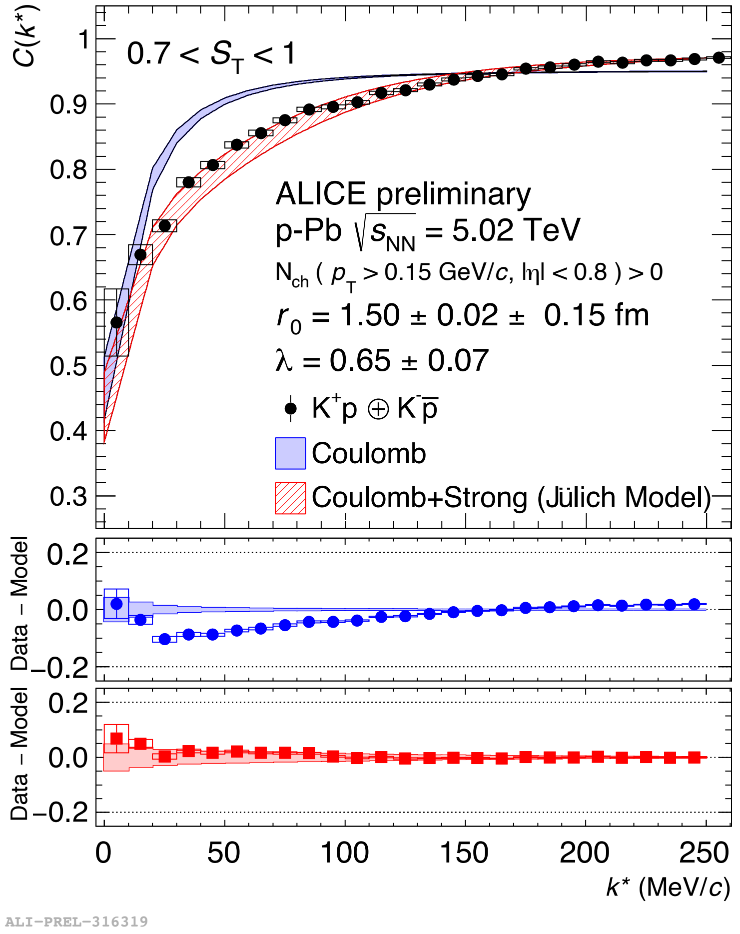

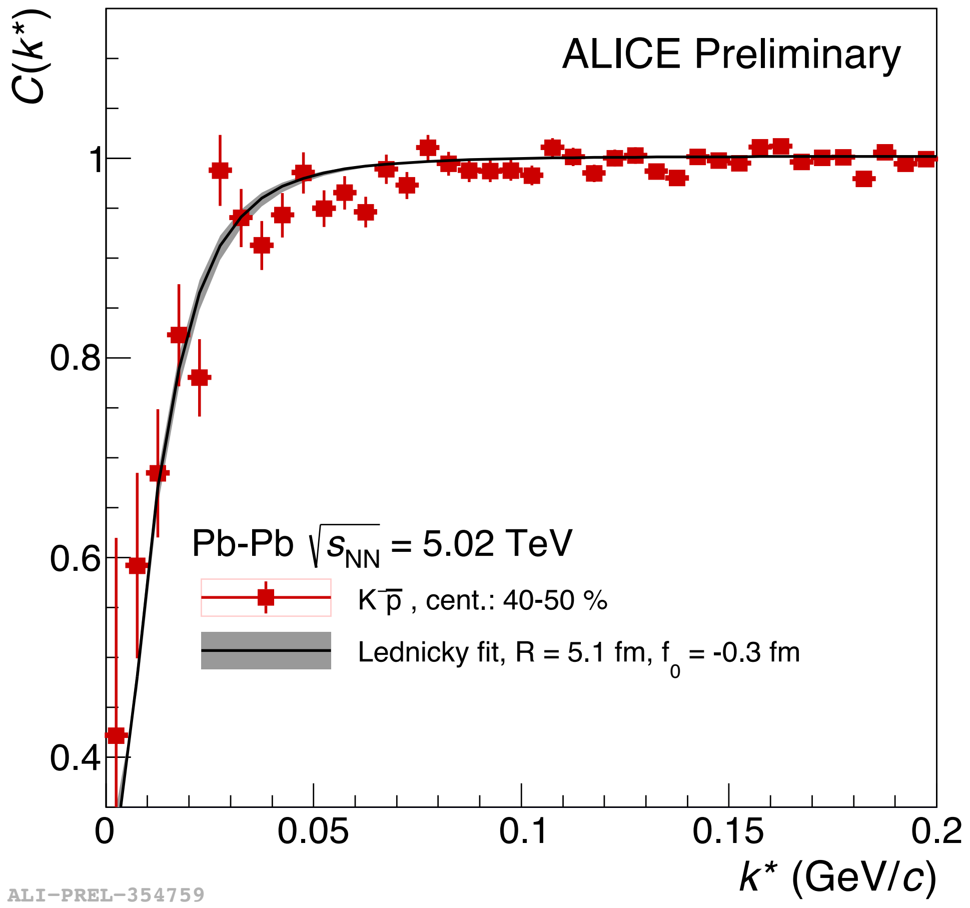

Lednicky´- Lyuboshits formula

$$C(k^*) = 1 + \sum_\sigma \rho_\sigma \left[\frac{1}{2} \left| \frac{f(k^*)}{R} \right|^2 \left(1 - \frac{d_0^\sigma}{2\sqrt{\pi}R} \right) + \frac{2\Re f(k^*)}{\sqrt{\pi}R} F_1(2k^*R) - \frac{\Im f(k^*)}{R} F_2(2k^*R) \right]$$

Meson-Baryon Lagrangian

$$P = \frac{1}{\sqrt{2}} \begin{pmatrix} \frac{\eta_N + \pi^0}{\sqrt{2}} & \pi^+ & K^+ \\ \pi^- & \frac{\eta_N - \pi^0}{\sqrt{2}} & K^0 \\ K^- & \bar{K}^0 & \eta_S \end{pmatrix} \quad B = \frac{1}{\sqrt{2}} \begin{pmatrix} \frac{\Lambda}{\sqrt{6}} + \frac{\Sigma^0}{\sqrt{2}} & \Sigma^+ & p \\ \Sigma^- & \frac{\Lambda}{\sqrt{6}} - \frac{\Sigma^0}{\sqrt{2}} & n \\ \Xi^- & \Xi^0 & -\frac{2\Lambda}{\sqrt{6}} \end{pmatrix} \quad \bar{B} = \frac{1}{\sqrt{2}} \begin{pmatrix} \frac{\bar{\Lambda}}{\sqrt{6}} + \frac{\bar{\Sigma}^0}{\sqrt{2}} & \bar{\Sigma}^- & \bar{\Xi}^+ \\ \bar{\Sigma}^+ & \frac{\bar{\Lambda}}{\sqrt{6}} - \frac{\bar{\Sigma}^0}{\sqrt{2}} & \bar{\Xi}^0 \\ \bar{p} & \bar{n} & -\frac{2\bar{\Lambda}}{\sqrt{6}} \end{pmatrix}$$

The Lagrangian describing the processes from B-antiB (p-antip, p-antiΛ, Λ-antiΛ) to Mesons-AntiMesons (π-antiπ, π-antiK) is typically written in the following form:

$$\mathcal{L} = g\mathrm{Tr}\{\mathrm{B} \cdot \bar{\mathrm{B}} \cdot \mathrm{P} \cdot \mathrm{P}\}$$

g is the coupling constant, same for all processes, typically determined by experiments (see e.g the nucleon-pion coupling $g_{\pi NN}$ from scattering data)

Scaling of the source in p-$\bar{\Lambda}$ and Λ-$\bar{\Lambda}$

- **Λ-antiΛ correlation function:** well reproduced by Lednicky-Lyuboshits (Pb–Pb), extracted radius in agreement with B-B scaling
- **p-antiΛ correlation function:** well reproduced by Lednicky-Lyuboshits, **BUT extracted radius larger wrt to B-B scaling**
- **Physical interpretation**: p-antiΛ is more coupled-channels contributions (supported by SU(3)$_f$ considerations) ⇒ larger amount of inelastic channels translates into larger radius

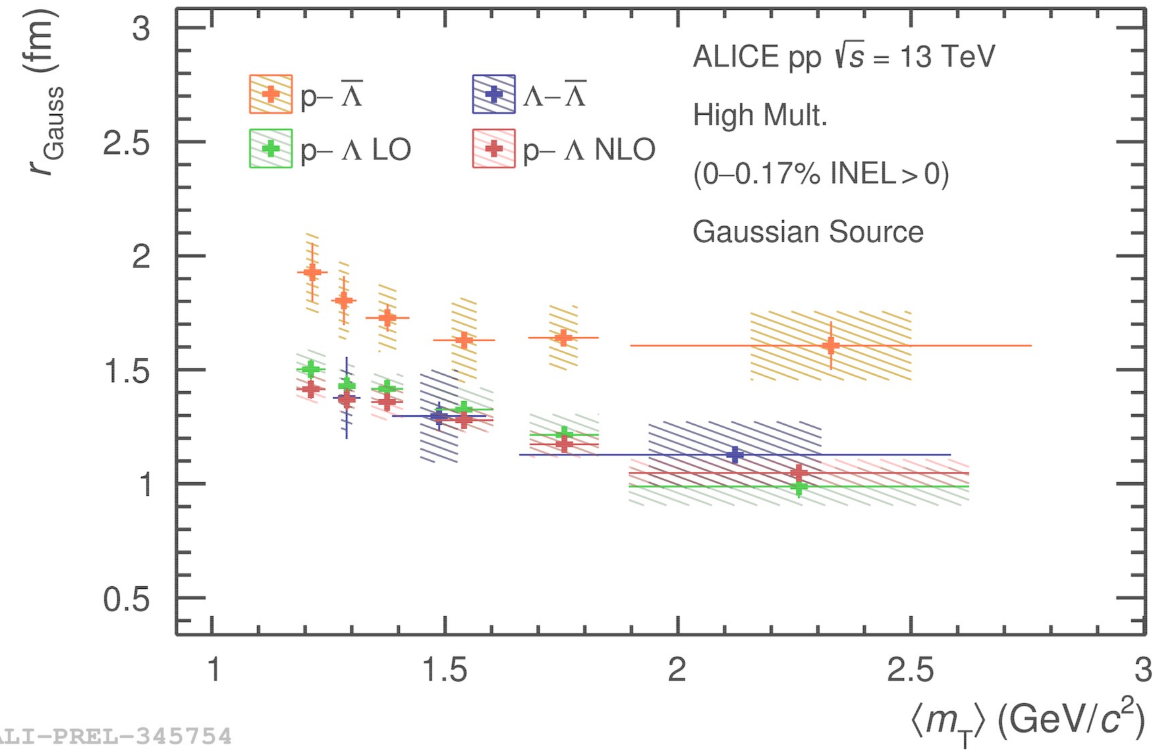

Mini-jet Background

- Large background that cannot be removed by applying S_T / S_0 cuts ⇒ results are obtained WITHOUT any S_T/S_0 cuts

- Use of Pythia to model the background:
  - jetty contributions ⇒ particles from Common ancestors
  - non-jetty part ⇒ particles from Non Common Ancestors

$$C_{mini-jet}(k^*) = [w_C C_C(k^*) + (1 - w_C) C_{NC}(k^*)]$$

- Weigths w_C to be fitted to data since they cannot be anchored to ΔηΔϕ correlations (more than a rescaling is needed)

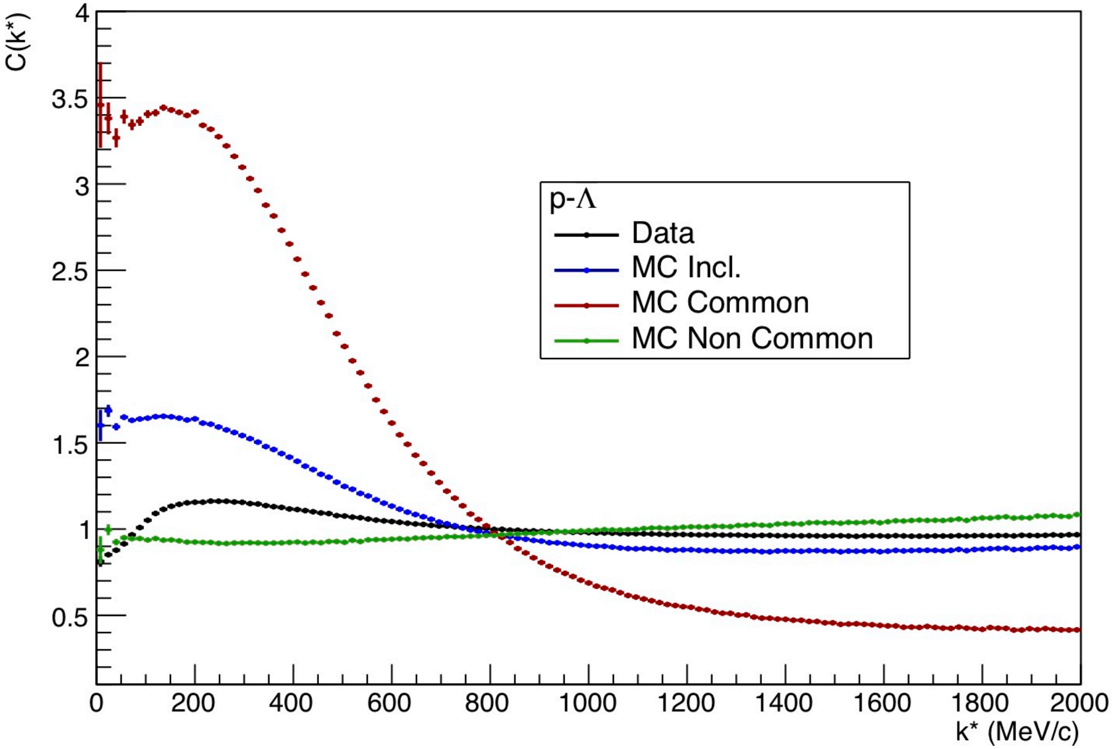

Fit procedure in B–$\overline{\mathrm{B}}$ femtoscopy

- Residual contributions included through λ parameters (DCA/CPA Template Fits)

- Non-femtoscopic background:
  - Mini-jet background ⇒ Shape fixed by Ancestors Template
  - Large k* kinematics effects ⇒ Pol1/Pol2 (prefit in k* [400-2500] MeV/c and kept fixed in the final fit)

$$C_{BCKG}(k^*) = [w_C C_C(k^*) + (1 - w_C) C_{NC}(k^*) + (a + bk^* + c(k^*)^2)]$$

- Total correlation function:
  - Free parameters: weigths w_C, Norm N_D
  - Coupled-channel modeling affects ONLY C_{model}

$$C_{tot}(k^*) = N_D \cdot C_{model}(k^*) \cdot C_{BCKG}(k^*),$$

Coupled channel wave functions

- Pairs close in mass with the same quantum numbers: e.g. p–Ξ^- and Λ–Λ
- Schrödinger equation of one pair → Equation system of all 1, … , N pairs

$$\hat{\mathcal{H}} \cdot \psi = \mathrm{E} \cdot \psi \mapsto \begin{pmatrix} \hat{\mathcal{H}}_{11} & \cdots & \hat{\mathcal{H}}_{1\mathrm{N}} \\ \vdots & \ddots & \vdots \\ \hat{\mathcal{H}}_{\mathrm{N}1} & \cdots & \hat{\mathcal{H}}_{NN} \end{pmatrix} \cdot \begin{pmatrix} \psi_1 \\ \vdots \\ \psi_N \end{pmatrix} = E \cdot \begin{pmatrix} \psi_1 \\ \vdots \\ \psi_N \end{pmatrix}$$

-

1) Coupled channels influence the elastic channels of the two-particle wave function ψ_j